DEVELOPMENT OF DIRECT-INVERSE 3-D METHOD
FOR APPLIED AERODYNAMIC DESIGN AND ANALYSIS

Semiannual Progress Report

July 1, 1986 - December 31, 1986

AEROSPACE ENGINEERING DEPARTMENT

TAMRF Report No. 5373-87-01

January 1987

NASA Grant No. NAG-1-619

TEXAS A&M UNIVERSITY

Leland A. Carlson
Professor of Aerospace Engineering
Texas A&M University
College Station, Texas 77843

TEXAS ENGINEERING EXPERIMENT STATION

DEVELOPMENT OF DIRECT-INVERSE 3-D METHOD FOR APPLIED AERODYNAMIC DESIGN AND ANALYSIS

Seminannual Progress Report

July 1, 1986 -- December 31, 1986

TAMRF Report No. 5373-87-01

January 1987

NASA Grant No. NAG-1-619

Leland A. Carlson
Professor of Aerospace Engineering
Texas A&M University
College Station, TX 77843

DEVELOPMENT OF A DIRECT-INVERSE 3-D METHOD FOR APPLIED TRANSONIC AERODYNAMIC DESIGN AND ANALYSIS

I. Introduction

This report covers the period from the July 1, 1986 thru December 31, 1986. The primary tasks during this period were the continued development of inverse design procedures for the TAWFIVE code, the development of corresponding relofting and trailing edge closure procedures, and the testing of the methods for a variety of cases.

II. Personnel

The staff associated with this project during the present reporting period were:

Leland A. Carlson, Principal Investigator

July thru August, Approximately 1/4 to 1/2 time

September thru December, Approximately 1/8 time

Thomas Gally, Graduate Research Assistant

July thru December

One-half time, Approximately 20 hours/week

The resarch work associated with this project will form the basis for the Masters thessis off Mr. Gally, who will receive his Masters degree in May 1987.

III. Research Progress

The work during the present reporting period is summarized in attached Appendix A. Appendix A is a copy of an extended abstract for a paper which has been submitted for presentation at the 5th Applied Aerodynamics Conference, August 17-19, 1987.

IV. Future Efforts

During the next reporting period it is anticipated that the inviscid portion of the effort will be concluded and that the work associated with including viscous corrections will be continued. Much of this work will involve the use of both fine and medium grids. Consquently, test cases will have to be selected in conjunction and consultation with individuals at NASA Langley. In addition, a proposal to continue the work for another year will be submitted.

GRANT MONITOR

The NASA Technical Monitor for this project is Richard L. Campbell, Applied Aerodynamics Group, NTF Aerodynamics Branch, Transonic Aerodynamics Division, NASA Langley.

APPENDIX A

INVISCID TRANSONIC WING DESIGN USING INVERSE METHODS IN CURVILINEAR COORDINATES

by

Thomas A. Gally* and Leland A. Carlson#

Aerospace Engineering Department

Texas A&M University

College Station, TX 77843

EXTENDED ABSTRACT

INTRODUCTION

In recent years the importance of transonic flight to both military and commercial aircraft and the development of specialized transonic wings for several flight research experiments has prompted significant efforts to develop accurate and reliable computational methods for the analysis and design of transonic wings. To date, most of the methods have been based upon the full potential approximation in either non-conservative or conservative form; and in the analysis case several excellent methods,[1-5] which include such effects as wing-body interaction, three-dimensional weak viscous interaction, and wake displacement thickness and curvature effects, have been developed. In particular, the TAWFIVE[5] code has proven to be an excellent and reliable analysis tool.[6-7]

---

* Graduate Research Assistant

Professor of Aerospace Engineering, Associate Fellow AIAA

In the area of design, most of the methods[8-15] which have attempted to automate the design process have also been based upon the full potential approximation; and these have usually utilized either the optimization or direct-inverse approach to determine a wing design. In the direct-inverse approach, the leading edge geometry of the wing is specified, which eliminates the need to specify a special boundary condition in the leading edge stagnation region. The wing geometry is then computed by specifying a desired pressure distribution over the remaining portion of the wing and then solving the mixed Neumann and Dirchlet boundary value problem by appropriate numerical techniques. The primary advantage of the method is that the input pressure distribution can be tailored to satisfy desired flight conditions such as a required pressure gradient to maintain a laminar flow or prevent boundary layer separation, a specified location and strength for the shock waves, or a certain span loading distribution, etc. In addition, since the approach is direct-inverse, such methods can be used entirely in the direct mode for aerodynamic analyses.

Because of its usefullness, the direct-inverse approach has been extensively investigated; and many codes have been developed and have established the validity of the method.[9-11,15] Unfortunately, these codes do not include many of the features which are necessary for efficient transonic design; and many contain significant approximations with respect to problem formulation and boundary conditions. In most cases, these approximations have not been verified sufficiently so as to have the confidence of the user community.

A desirable feature in any wing design program is the ability to determine the wing geometry subject to various spanwise and chordwise physical constraints. Figure 1 shows several possible design situations in which only part of the wing needs to be or possibly can be designed or modified. Thus, a design program

should have both analysis and design capability; and it should permit extensive freedom in selecting which regions are to be designed and which are to be analysed. In addition, since it must handle both analysis and design, it should be computationally consistent. In other words, if the design portion yields a certain shape for a given pressure distribution, the analysis section should reproduce the original pressure distribution using the designed shape. Further, a good design code should permit the user to specify the trailing edge thickness at the design span stations.

Another desirable feature in any transonic wing design method is the option to include weak viscous interaction effects resulting from the viscous wake and the three dimensional boundary layer on the wing. Unfortunately, at transonic speeds, experimental and flight test evidence[4] indicates that wing and wake viscous interaction effects can significantly affect both the pressure distribution on a wing and the resultant aerodynamic force coefficients. To prevent serious discrepancies, the effects of the three dimensional laminar-turbulent boundary layer and the wake, particularly when only part of the wing is being designed and the rest is being analyzed, should be included in any transonic analysis-design numerical method. Unfortunately, previous methods, such as those in Ref. 9-11 and 15, often only include turbulent viscous interaction and ignore wake effects. In addition, the turbulent models are usually of the two-dimensional strip type modified for quasi-three dimensional effects; and they have not been extensively verified.

Another factor which is important in transonic wing design is the interaction between the wing and the body. Unfortunately, most transonic wing design codes do not include wing body effects; and those that do, do so approximately or are limited in the types of body shapes.[16] In this respect, analysis codes such as

TAWFIVE[4-5] are considerably better in that they have the ability to accurately model arbitrary non-axisymmetric fuselage cross sections.

Based upon the items discussed above, a research program has been initiated to expand and develop the TAWFIVE three dimensional finite volume fully conservative potential flow analysis code into a transonic wing design method based upon the direct-inverse approach. Since TAWFIVE already includes the effects of laminar-turbulent boundary layer interaction, wake thickness and curvature, and arbitrarily shaped bodies, and since it has been extensively tested and verified[4-7], it is a logical candidate for this effort. The specific objectives of the present program are as follows:

(1) Develop an inverse wing design method and code which is suitable for applied aerodynamic studies, which is applicable to wing planforms having a wide range of spanwise and chordwise constraints, which contains a method for controlling trailing edge closure, and which includes wing-body interaction effects.

(2) Extend the method and code to include viscous interaction and wake curvature effects.

Since the viscous interaction studies are currently in their initial stages, the proposed paper will only present the method and example results associated with the first objective.

PROBLEM FORMULATION

As indicated above, the primary tasks associated with the present investigation have been to modify the inviscid portion of the TAWFIVE code to handle inverse boundary conditions and to develop a suitable means of computing

the wing ordinates from the resultant inverse solution. The inviscid portion of TAWFIVE solves the full potential flow equation in conservative finite volume form in a body fitted cylindrical wind tunnel coordinate system (sometimes referred to as a body fitted, sheared, parabolic system); and it is essentially a slightly modified verision of the original FLO30 code. Since the fundamental equations, numerical formulation, and treatment of boundary conditions in direct (analysis) regions where the surfaces are specified are unchanged in the present problem, details concerning these topics will not be presented here. Complete information concerning TAWFIVE and FLO30 is presented in References 1-5.

Inverse Pressure Boundary Condition Specification

In the inverse design regions, such as those shown on Figure 1, the pressure coefficient, C_p, must be specified on the wing surface as the boundary condition for the full potential equation. By using the full potential pressure coefficient expression

$$C_p = \frac{2}{\gamma M_\infty^2}\left\{\left[1+\frac{\gamma-1}{2}M_\infty^2\left(1-\frac{Q^2}{q_\infty^2}\right)\right]^{\frac{\gamma}{\gamma-1}}-1\right\}$$

where $Q^2 = u^2+v^2+w^2$

$$\frac{u}{q_\infty} = \phi_x\cos\alpha \qquad \frac{v}{q_\infty} = \phi_y + \sin\alpha \qquad \frac{w}{q_\infty} = \phi_z$$

and u, v, and w are the Cartesian chordwise, vertical, and spanwise velocity components respectively,, ϕ_x can be obtained in terms of the pressure coefficient as

$$\phi_x = \frac{1-\frac{\gamma-1}{2}M_\infty^2\left[\left(1+\frac{\gamma M_\infty^2 C_p}{2}\right)^{\frac{\gamma}{\gamma-1}}-1\right]}{1+\left(\frac{v}{u}\right)^2+\left(\frac{w}{u}\right)^2}-\cos\alpha$$

This approach is the formulation previously used in Ref. 11, 15, and 16, which used the ZEBRA II solution algorithm and a sheared Cartesian coordinate system.

However, TAWFIVE uses a body fitted curvilinear coordinate system which requires recasting of the above equation.

The velocities can be expressed in the physical plane (x,y,z) and in the computational space (ξ,η,ζ) as

$$\begin{pmatrix} u \\ v \\ w \end{pmatrix} = \begin{pmatrix} \phi_x \\ \phi_y \\ \phi_z \end{pmatrix} + \begin{pmatrix} \cos\alpha \\ \sin\alpha \\ 0 \end{pmatrix} = [J]^T \begin{bmatrix} \phi_\xi \\ \phi_\eta \\ \phi_\zeta \end{bmatrix} + \begin{pmatrix} \cos\alpha \\ \sin\alpha \\ 0 \end{pmatrix}$$

$$[J] = \begin{bmatrix} \xi_x & \xi_y & \xi_z \\ \eta_x & \eta_y & \eta_z \\ \zeta_x & \zeta_y & \zeta_z \end{bmatrix}$$

Thus, ϕ_x solved for above from the pressure coefficient equation is equivalent to

$$\phi_x = J_{11}\phi_\xi + J_{21}\phi_\eta + J_{31}\phi_\zeta$$

Several methods have been investigated for evaluating this expression and, hence, for specification of the inverse boundary condition. It is anticipated that several of these will be discussed in the final paper and the advantages and disadvantages of each indicated. For the results presented here, the pressure coefficient in design regions is specified at grid midpoints (I+1/2, J, K) on the current wing surface. The expression for ϕ_x is then

$$\phi_x = \xi_x\left(\phi(I+1)-\phi(I)\right)_{JK} + \frac{\eta_x}{2}\left(3\phi(J)-4\phi(J+1)+\phi(J+2)\right)_{I+1/2,K} + \frac{\zeta_x}{2}\left(\phi(K+1)-\phi(K-1)\right)_{I+1/2,J}$$

where the metrics, ξ_x, η_x, ζ_x and , are considered constants for a given grid. (As will be mentioned later, the grid changes during the solution.) In this approach, as the calculations proceed downstream from the analysis regions near the leading edge into the inverse regions, the upstream point $\phi(I)$ is known. The values of the metrics and the cross flow derivatives are found by averaging the values from the points I and I+1. In this approach, the only unknown is $\phi(I+1)$

and it can be obtained explicitly. It is believed that this formulation is preferable to other possibilities, such as specifying the pressure coefficient at grid points (I,J,K), since it strongly couples the potential at (I+1) to the immediate upstream point and eliminates any decoupling between alternating points. Additional details will be presented in the final paper.

In the above inverse boundary condition treatment, the velocity ratios v/u and w/u are considered known. Since the value of these terms only slightly affect the value of the inverse boundary condition, their values are lagged in the solution and only periodically updated.

Design Surface Calculation

As the inverse boundary conditons drive the flowfield to a converged solution, the new displacement surface corresponding to the specified pressure boundary conditions needs to be calculated periodically in order that the prescribed pressures are imposed at the proper location. Each new surface can be found by integration of the local wing slopes which are computed from the flow tangency boundary condition, i.e.

$$\left(\frac{\partial n}{\partial s}\right)_{wing} = \frac{V}{U} - \frac{W}{U}\frac{\partial n}{\partial s}\Big|_{wing}$$

The above equation is written in the wing body curvilinear coordinate system using contravariant velocities and is a direct analogy to the boundary condition expressed in physical space. In order to solve the above equation for the wing slope, $\partial n/\partial s$, it is necessary to lag the cross-flow slopes, $\partial n/\partial s$, using their values from the previous surface update. Since the grid is, after each update, assumed to be surface fitted, these values are convienently zero. Thus, the equation for the slopes of the new surface is

$$\left.\frac{\partial \eta}{\partial \xi}\right|_{wing} = \frac{V}{U}$$

Integration of these slopes yields a $\Delta\eta$ for the new surface relative to the old location. This change is converted to a physical displacement approximately normal to the wing surface using the local transformation metrics of the grid. The sum of the physical displacements at each point from each surface update are then stored and used in the same manner as the code uses boundary layer displacement thicknesses to update and create a new grid.

For simplicity, the contravariant velocities used in the slope equation are evaluated only at the previous displacement surface where the pressure distributions are specified. This approach means that the slope equations are not exact because the velocities should be evaluated at the new surface boundary. However, as the solution converges the changes in the surface locations for the final few surface updates are small, and the present approach should lead to converged accurate surface ordinates.

Obviously, the accuracy of the surface calculation depends upon the accuracy of the contravariant velocity calculations. After trying several approaches, it has been found that the most accurate and/or consistent approach is to use the residual equation and assume that the residual is zero on the current displacement surface boundary (i.e. assume that the solution has converged). The resultant expression yields V/U and requires knowledge of all flow variables at cell centers above the surface, which can be calculated, and all values except oV at the "ghost"cell centers inside the wing surface, which are not known in the inverse region. If, however, the values inside the surface are obtained using the tangency boundary condition, only a small error is introduced; and this error

approaches zero as the updated grid surface converges to the design surface. Additional details will be presented in the final paper.

While the above approach should yield wing ordinates which are consistent with the specified pressure boundary conditions, there is no guarantee that the trailing edge of the designed wing will be "closed"; and in fact it may be extremely blunt or, conversely, fish-tailed. Since an extremely blunt or open trailing edge is undesirable and a fish-tailed surface is physically impossible, some mechanism for controlling trailing edge closure must be included in the formulation. Fortunately, Weed et al[11] has shown that closure can be controlled by linearly relofting or rotating the direct leading edge region to force the trailing edges to either specified locations or to a fixed thickness.

In the present formulation two types of relofting have been implemented. The first is associated with a case in which the user specifies either closure, a trailing edge thickness distribution, or the values of the trailing edge ordinates. Thus, it is activiated only by user choice; and such relofting is termed "forced". On the other hand, if during a surface update the new trailing edge at any span station is fish-tailed, the grid generation scheme will fail when it trys to compute a new grid corresponding to the fish tail shape. To prevent such failures, a second type of relofting is included which is automatically activated whenever fish-tailing or excessive openess occurs. (The final paper will discuss the relofting procedures in more detail.) It should be noted that any time relofting is activated, the leading edge region of the design stations is slightly changed from that which was originally specified.

These techniques for specifying the inverse pressure boundary condition, determining the design surface shapes, and including relofting whenever desired or required have been incorporated into the TAWFIVE code. For fine grid results,

the resulting program can be efficiently run on either large mainframe computers or midsize mini-computers. For medium grid results, the program can also be run on PC/AT class microcomputers.

TYPICAL RESULTS

In this section results from five different test cases for both subcritical and supercritical conditions will be presented. These cases are not intended to be definitive or even representative of practical designs but have been selected as examples of the capability of the present inverse design technique. The results shown were obtained on a medium grid having 81 streamwise, 13 vertical, and 19 spanwise points with 11 spanwise stations and 53 points on the wing at each station; and in all cases the maximum change in the reduced potential was reduced at least three orders of magnitude. Thus, the results do not represent ultimate convergence but should be representative of "engineering accuracy".

The planform selected for the test cases was the Lockheed Wing A wing-body. The wing for this configuration has a quarter chord sweep of 25 deg., a linear twist distribution ranging from 2.28 deg. at the wing body junction to -2.04 deg. at the wing tip, an aspect ratio of eight, and a taper ratio of 0.4. The last two values are based upon the wing without fuselage. However, instead of the supercritical sections normally associated with Wing A, the initial airfoil sections at each span station were assumed to NACA 0012 airfoils.

The target pressure distributions used in the design regions were selected to yield airfoil shapes thicker in the aft portions of each section; and, at supercritical conditions, to yield on the upper surface weaker and more forward shock waves than those which would normally occur on a NACA 0012 section. On

the lower surface, the target pressure distributions were selected to have either a favorable pressure gradient or fairly constant pressure plateau over much of the lower surface.

All subcritical cases were for a freestream Mach number of 0.7 and an angle of attack of two degrees. In each case, the pressure distribution was specified in the design regions from the 15% local chord location to the trailing edge and used as the boundary condition in these inverse regions starting with the first iteration. Normally, two hundred SLOR iterations were executed prior to the first design surface update calculation; and subsequently, surface updates were computed every fifty cycles. Usually, the solution was considered converged and terminated after 450 total iterations.

Supercritical cases followed a similar procedure except that the freestream Mach number was 0.8. Again the angle of attack was two degrees. However, for these cases three hundred iterations were performed prior to the first surface update calculation in order to better resolve the leading edge pressure distribution in design regions. Because of the upstream dependance of the flowfield, particularly for the supercritical cases, it was determined to be essential to obtain a good computational solution in the leading edge region before any surface updates. Otherwise the initial surface changes were so drastic that a large number of additional surface calculations, and accompanying iterations, were necessary in order to achieve convergence.

Finally, for those cases where trailing edge closure was specified by the input, forced relofting was not performed until the second surface update. This approach was used because the first surface update usually involved large changes in the surface shape, and it was believed that attempting to force closure at the same time might lead to convergence difficulties.

Test Case A

As shown on Figure 2, the objective of Case A was to modify only the upper surface between 45% and 85% semi-span. As indicated above, the input pressure distribution for the design region corresponded to that of a wing composed of airfoil sections which were thicker than a NACA 0012 in the aft portion of each section; and these pressures were previously obtained with a corresponding analysis computation. Thus, since this case also required trailing edge closure, Case A was test of the ability of the method to reproduce the airfoil sections of a known wing. Both subcritical, designated Case A1, and supercritical, designated Case A2, solutions were obtained.

The resultant designed airfoil sections for the case having a subcritical freestream are shown on Figure 3. As can be seen, the designed sections are considerably different than the original NACA 0012 airfoils; and they are in reasonable agreement, even on the expanded scale, with the target sections. However, there are some slight discrepencies at the boundary stations at 50 and 80% semi-span. It is believed that these are due to a combination of terminating the computations prior to ultimate convergence and to the significant variation in spanwise slope near the trailing edge resulting from the change between the NACA 0012 sections in the analysis zones to the designed airfoils in the inverse regions. Nevertheless, it is believed that the agreement between the designed surfaces and the target surfaces is adequate.

The true test, however, of an inverse wing design method is not its ability to reproduce "known" airfoil sections but rather a comparison between the target pressure distributions used to design the wing and those computed by an analysis of the designed wing. Figure 4 presents such a comparison for subcritical Case A1; and, as can be seen, the analysis results for the designed wing (labeled

"designed surface pressures") are in excellent agreement with the target pressures as are the local lift coefficients.

Figures 5 and 6 show similar section profiles and pressure distributions for Case A at supercritical conditions. Again the agreement between the designed surfaces and the target surfaces and the pressures from an analysis of the designed wing and the target pressures are excellent. It is believed that Figures 3-6 demonstrate that the current method can be used to modify the design of the upper surface of a wing mounted on a body.

Test Case B

This case, which is depicted on Figure 7, was created to test the ability of the method to design both upper and lower surfaces. Subcritical (Case B1) and supercritical (Case B2) results are shown on Figures 8-11. As in the previous case, trailing edge closure was required; and as a result the designed surface shapes have the same character as those for Case A in that there is good agreement at the inner stations but slight discrepencies between the designed surfaces and the target sections at the boundary stations. However, as shown on Figures 9 and 11, there is still excellent agreement between the pressures computed by an analysis of the designed wings and the desired target pressures used in the inverse design. Thus, it can be concluded that the method can be used to modify the design of the upper and lower surfaces of a wing mounted on a body.

Test Case C

The inverse design regions for Case C, which was an attempt to design both upper and lower surfaces on two noncontiguous regions of the wing at supercritical conditions, are shown on Figure 12; and a comparison between the initial pressure distribution associated with NACA 0012 sections and the target pressures is portrayed on Figure 13. As can be seen, the target pressure

distribution essentially eliminates at inboard stations the upper surface shock wave present on the original wing; and at outboard stations it weakens the shock and moves it forward. In addition, significant changes in the lower surface pressure gradients are evident. Also shown on Figure 13 are the pressures computed by the program at the end of the inverse design procedure (denoted as "design pressures"). These pressures are in excellent agreement with the target pressures, which indicates that the method is satisfying properly the desired inverse boundary conditions.

The corresponding designed airfoil sections for this case are shown on Figure 14. Even on the expanded scale, the agreement between the designed and target surfaces is excellent at all design stations. However, trailing edge closure was not enforced for this case and there is at the boundary stations some departure between the designed surfaces and the target surfaces near the trailing edge. Again it is believed that this slight difference is a ramification of the change in spanwise slopes near the trailing edge between the direct and inverse regions.

In any event, the pressure distributions resulting from an analysis of the designed surfaces shown in Figure 14 are in excellent agreement with the target pressures, as can be seen on Figure 15. In addition, the section lift coefficients at the various design stations are in very good agreement with the target coefficients. Based upon these results it is believed that the present method can adequately design/modify nonadjacent regions of a wing in transonic flow.

Test Case D

As shown on Figure 16, Case D involved the inverse design of the entire wing on both the upper and lower surfaces. In addition, as depicted on Figure 17, the initial twist distribution was constant from the root to 40% semi-span followed by a linear distribution between 40% and the wing tip; and the inverse pressure

distribution was selected to correspond to an approximately linear twist distribution between the root and the tip. Thus, this case was a test of both the ability of the method to design an entire wing and to modify the twist distribution. Obviously, since the twist had to be permitted to vary, trailing edge closure was not required. Also, the results shown are for supercritical conditions.

As can be seen on Figure 17, the twist distribution resulting from the design calculation, while considerably different than the initial distribution, is slightly different than the target distribution. This difference occurred for several reasons. First, in the current version of the program the wing section at the root-body junction cannot be inversely designed. Thus, when designing the entire wing, the program automatically makes the root section nondimensionally identical to that at the first span station; and the twist at the root and at the 10% semi-span station are identical. Second, the leading edge shapes in the direct region forward of 15% chord correspond to the initial shapes and are oriented by the initial twist distribution. Thus, they do not correspond to those associated with the target twist. Consequently, if the method correctly matches the input pressure distribution in the inverse region from 15% chord aft, it should yield slightly different pressures near the leading edge and a slightly different final twist distribution.

Figures 18(a-b) compare the designed airfoil sections with the original surfaces. Due to the manner in which these plots were constructed, if the trailing edge of a designed surface is above that of the corresponding original surface, then that design station has a lower twist angle than the initial twist. As can be seen from Figures 17 and 18, the designed wing is considerably different than the original and has an almost linear twist distribution.

As indicated above, the only way a design can be validated is to analyse the designed wing and compare the resultant pressures in the inverse regions with the target values. Figures 19(a-b) present such a comparison for Case D, and it is apparent that the present direct-inverse method did design a wing having the appropriate pressures in the inverse regions aft of 15% chord. However, as should be expected, since the leading edge regions were different than those corresponding to a true linear twist case, the pressure distributions in the leading edge regions and the section lift coefficients were slightly different than those of the target case. (The target lift coefficients were obtained by an analysis of the target section shapes with a linear twist distribution.) It is believed that the results shown on Figure 19 demonstrate that the present method can be used to design an entire wing in supercritical flow.

Test Case E

As a final test case, it was decided to design two non-adjacent upper surface regions simultaneously with a lower surface region which overlapped the upper zones. The location of these inverse design regions is shown on Figure 20. Likewise, Figure 21 compares the pressures associated with the initial wing section shapes to the target pressures and to the pressures computed at the end of the design calculation. It should be noted that this case is for supercritical conditions and trailing edge closure is not enforced. As can be seen, at stations where only one surface is being designed (e.g. 20%, 40%, 50%, 70%) the pressure distribution on the fixed surface also changes due to three dimensional effects from adjacent stations which have been redesigned. However, as depicted on Figure 22, only the design surfaces change from the original shape; and these surfaces are in reasonable agreement with the target profiles.

Finally, Figure 23 compares analysis results obtained for the designed wing with the target pressures. Even for this complicated case, the agreement between the two distributions and between the actual and target lift coefficients is excellent.

CONCLUSION

A direct-invese transonic wing design method based upon the TAWFIVE computer code has been developed. This method includes the effects of wing body interaction and at subsonic and transonic conditions is capable of designing/modifying wings subject to a variety of spanwise and chordwise constraints. A series of results have been presented which demonstrate the utility and versatility of the method.

ACKNOWLEDGMENTS

The work presented in this paper was primarily supported by the National Aeronautics and Space Administration under Grant NAG-1-619 with Richard L. Campbell of the Langley Research Center as technical monitor. The authors express their appreciation to Richard L. Campbell and Edgar Waggoner of NASA Langley for the assistance and helpful suggestions.

REFERENCES

1. Jameson, A. and Caughey, D. A., "A Finite Volume Method for Transonic Potential Flow Calculations," Proceedings AIAA 3rd Computational Fluid Dynamics Conference, Albuquerque, NM, June 1977, pp. 35-54.

2. Caughey, D. A. and Jameson, A., "Numerical Calculation of Transonic Potential Flow about Wing-Body Combinations," AIAA Journal, Vol. 17, No. 2, February 1979, pp. 175-181.

3. Caughey, D. A. and Jameson, A., "Progress in Finite-Volume Calculations for Wing-Fuselage Combinations," AIAA Journal, Vol. 18, No. 11, November 1980, pp. 1281-1288.

4. Streett, C. L., "Viscous-Inviscid Interaction for Transonic Wing-Body Configurations Including Wake Effects," AIAA Journal, Vol. 20, No. 7, July 1982, pp. 915-923.

5. Melson, N. D. and Streett, C. L., "TAWFIVE:A User's Guide," NASA TM84619, September 1983.

6. Waggoner, E. G., Phillips, P. S., Viken, J. K., and Davis, W. H., "Potential Flow Calculations and Preliminary Wing Design Support of an NLF Variable Sweep Transition Flight Experiments," AIAA Paper No. 85-0426, January 1985.

7. Campbell, R. L., E. G. Waggoner, and Phillips, P. S., "Design of a Natural Laminar Flow Wing for a Transonic Corporate Transport," AIAA Paper No. 86-0314.

8. Lores, M. E. and Hinson, B. L., "Transonic Design Using Computational Aerodynamics," Progress in Aeronautics and Astronautics, edited by D. Nixon, Vol. 22, AIAA, NY, 1982, pp. 377-398.

9. Henne, P. A., "Inverse Transonic Wing Design Method," Journal of Aircraft, Vol. 18, Feb. 1981, pp. 121-127.

10. Shankar, V., Malmuth, N., D., and Cole, J. D., "Computational Transonic Design Procedure for Three Dimensional Wings and Wing Body Combinations," AIAA Paper 79-0322, Jan. 1979.

11. Weed, R. A., Carlson, L. A., and Anderson, W. K., "A Combined Direct Inverse Three Dimensional Transonic Wing Design Method for Vector Computers," AIAA Paper 83-2156, Aug., 1984.

12. Bauer, F., Garabedian, P., and McFadden, G., "The NYU Inverse Swept Wing Code," NASA CR-3662, January 1983.

13. Consentino, G. B., and Holst, T. L., "Numerical Optimization Design of Advanced Transonic Wing Configurations," AIAA Paper 85-0424, January 1985.

14. Davis, W., "TRO-2D: A Code for Rational Transonic Aero Optimization", AIAA Paper 85-0425, January 1985.

15. Carlson, L. A. and Weed, R. A., "Direct-Inverse Transonic Wing Analysis-Design Method with Viscous Interaction," Journal of Aircraft, Vol. 23, No. 9, Sept 1986, pp. 711-718.

16. Weed, R. A., and Carlson, L. A., "Combined Direct/Inverse Three Dimensional Wing Design with Viscous and Wing Body Effects," David Taylor Naval Ship Research and Development Center, Bethesda, MD, DTNSRDC-ASED-CR-02-84, Feb. 1986.

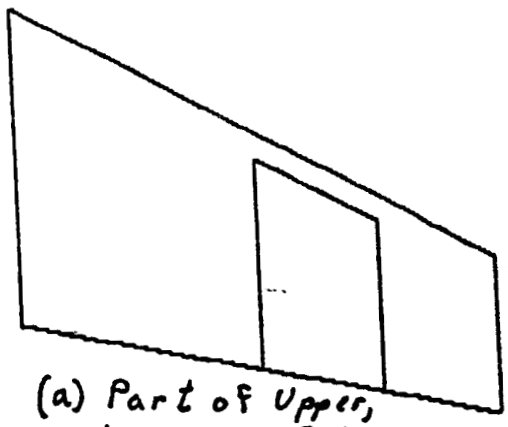

(a) Part of Upper, Lower, or Both

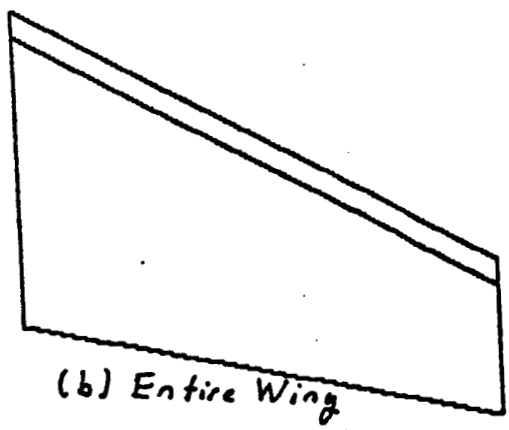

(b) Entire Wing

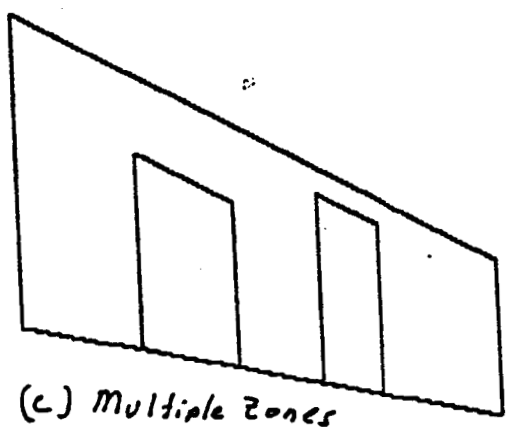

(c) Multiple Zones

Figure 1 -- Possible Design Situations

Figure 2 -- Inverse Design Regions for Case A

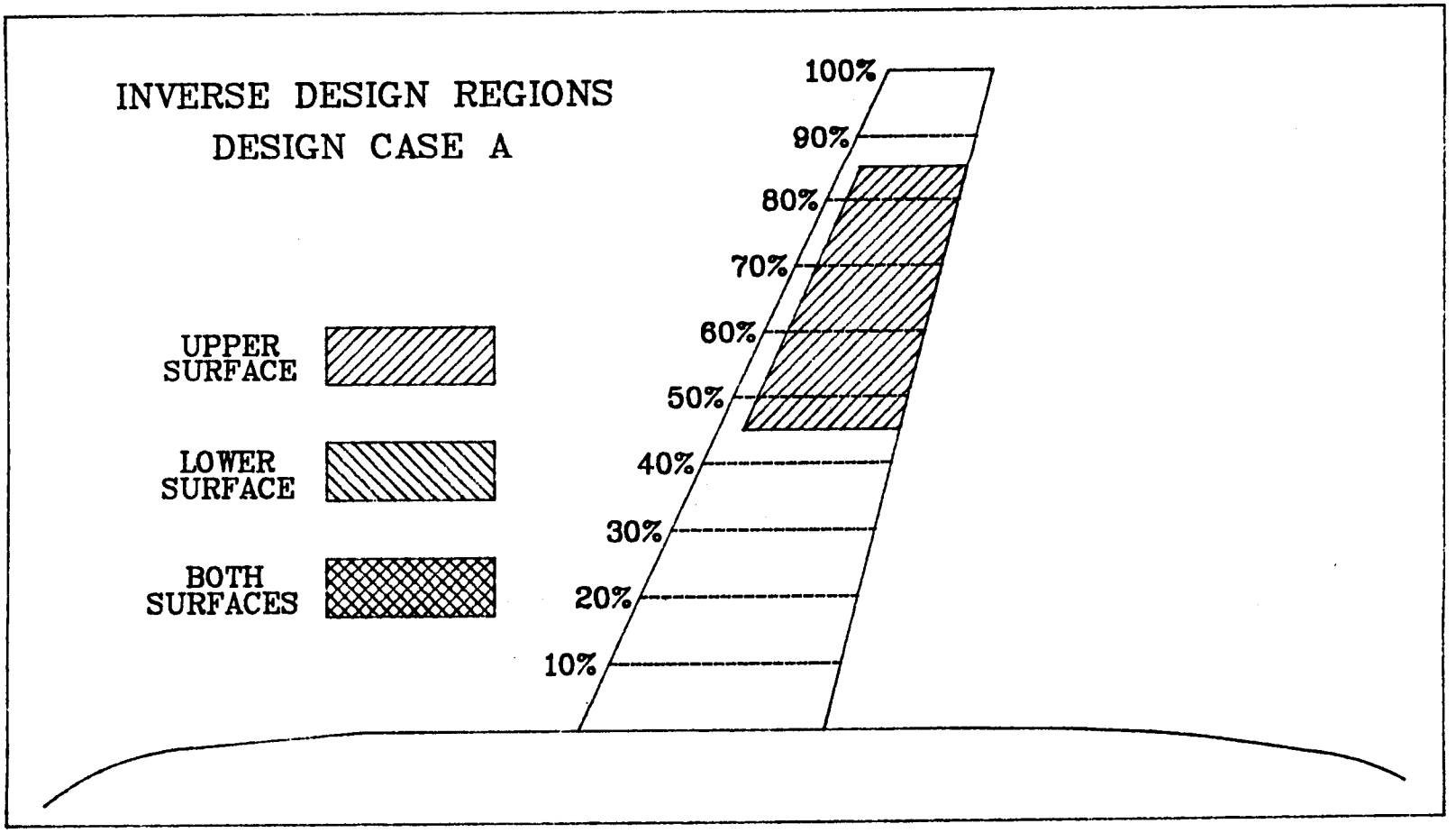

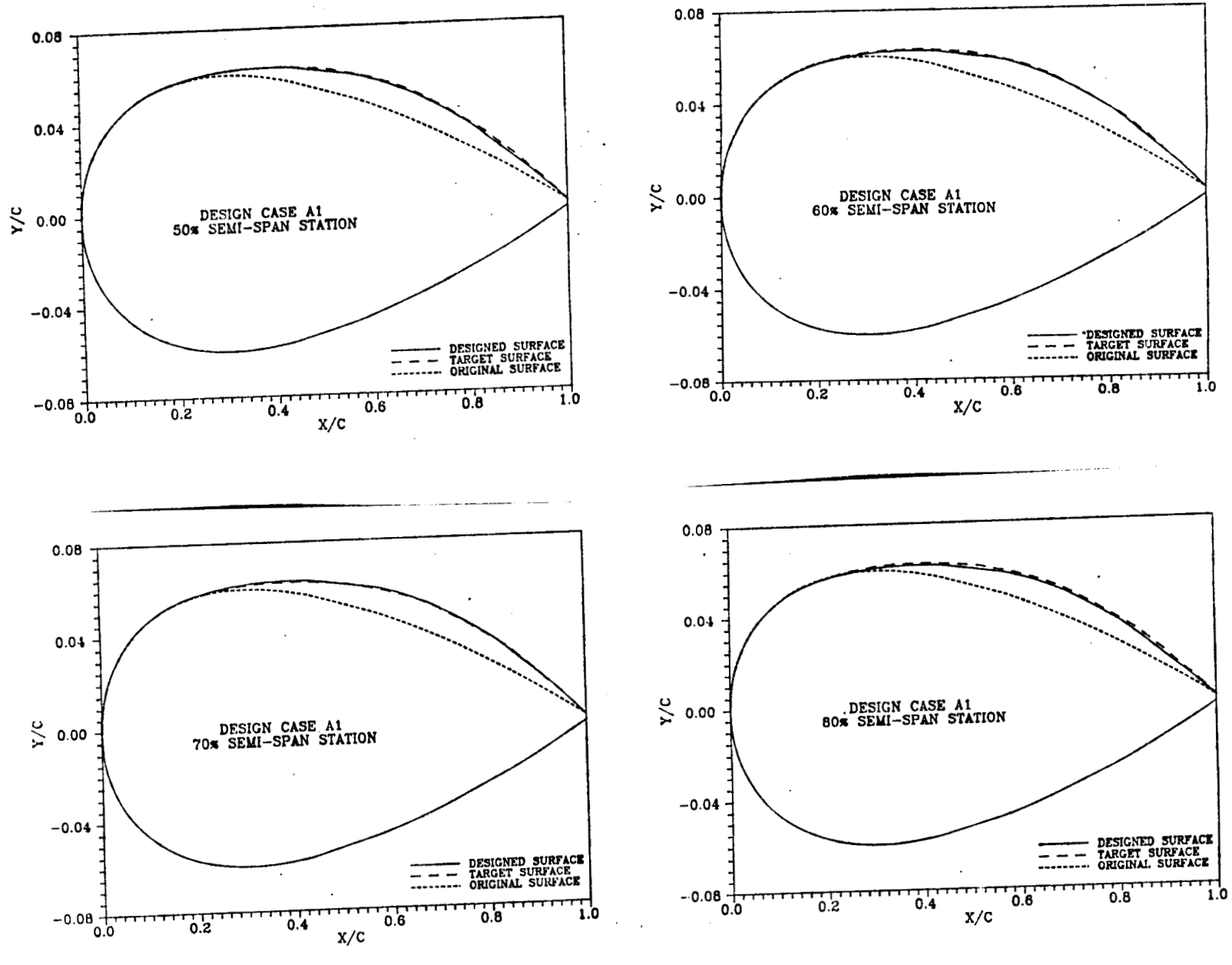

Figure 3 -- Comparison of Designed Sections with Original and Target Sections (Case A1)

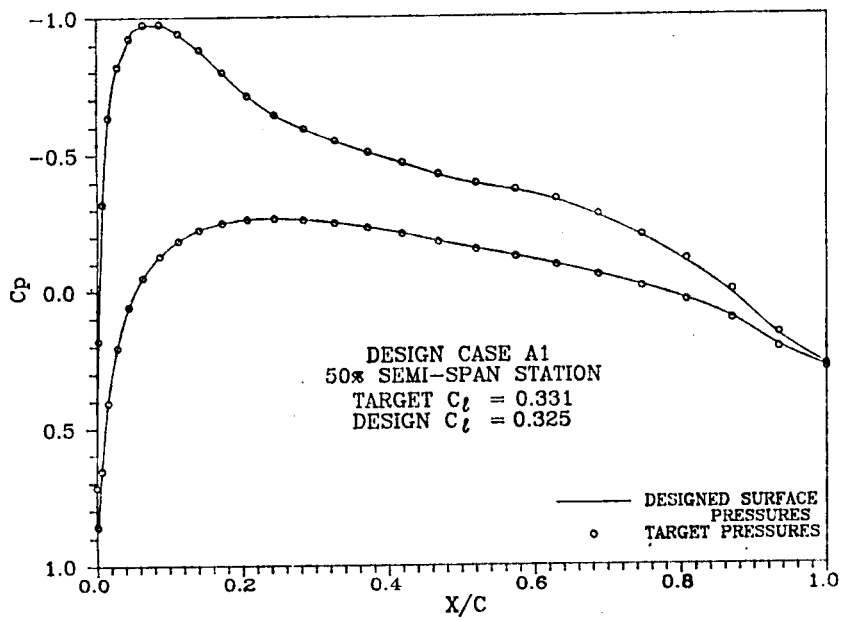

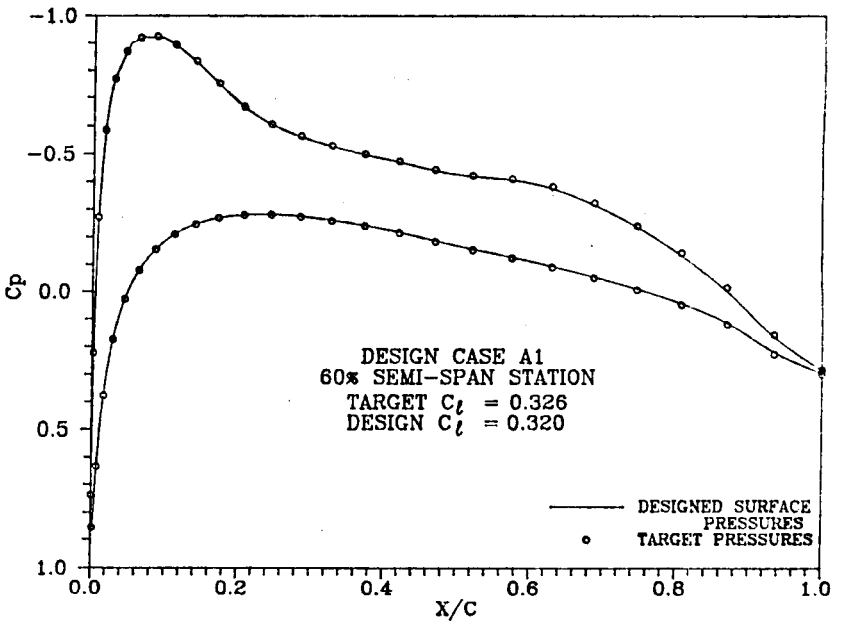

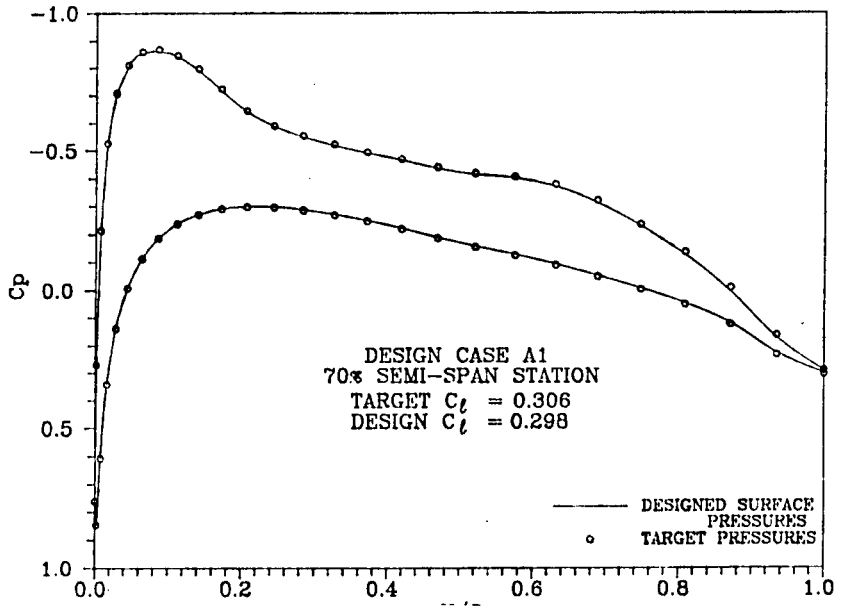

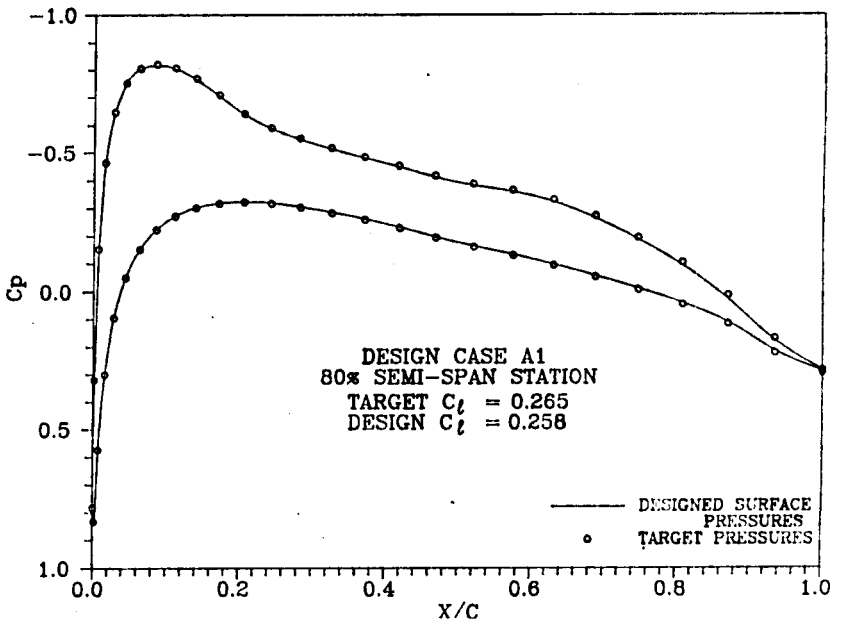

Figure 4 -- Comparison of Pressures from Analysis of Designed Wing with Target Distributions (Case A1)

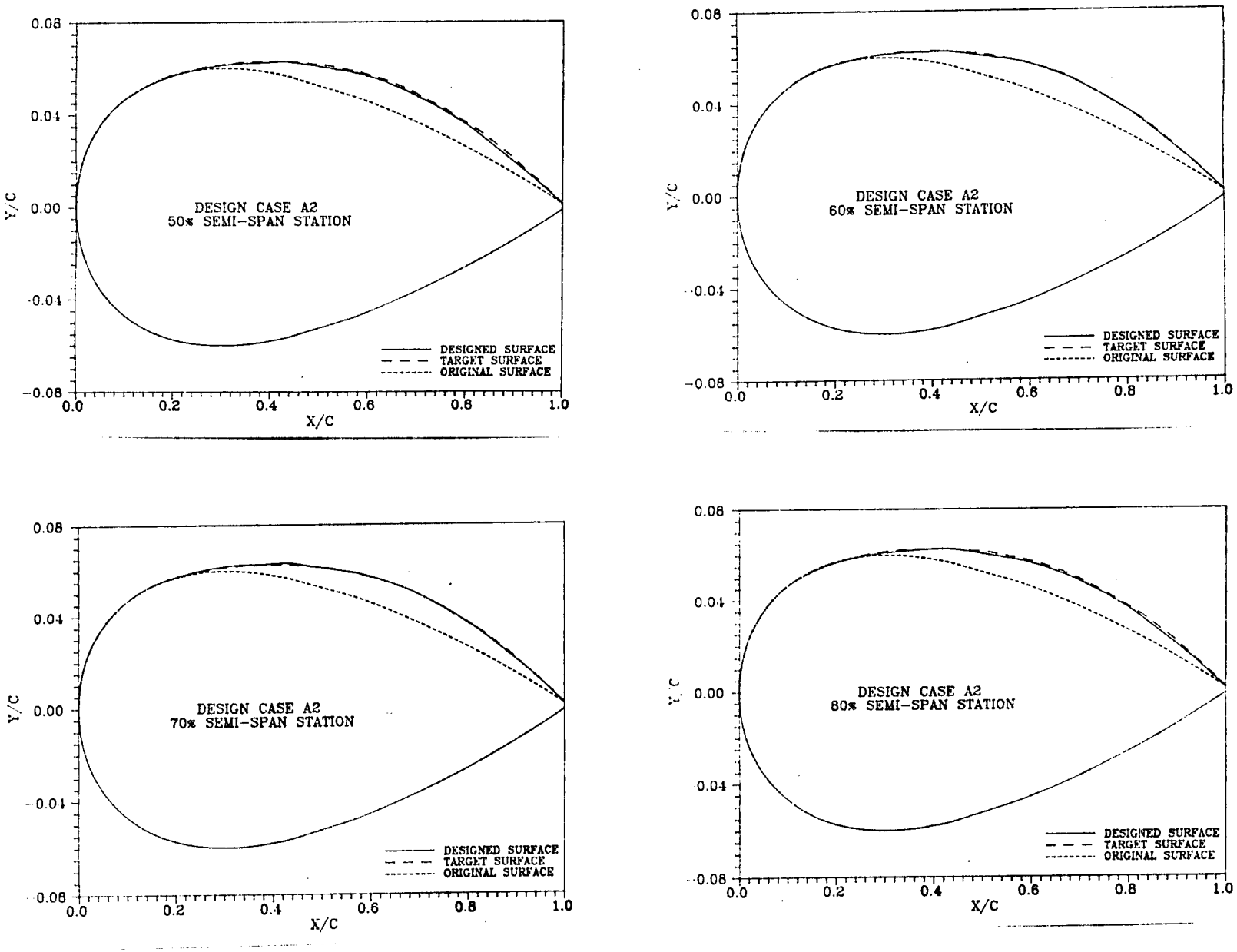

Figure 5 -- Comparison of Designed Sections with Original and Target Sections (Case A2)

Figure 6 -- Comparison of Pressures from Analysis of Designed Wing with Target Distributions (Case A2)

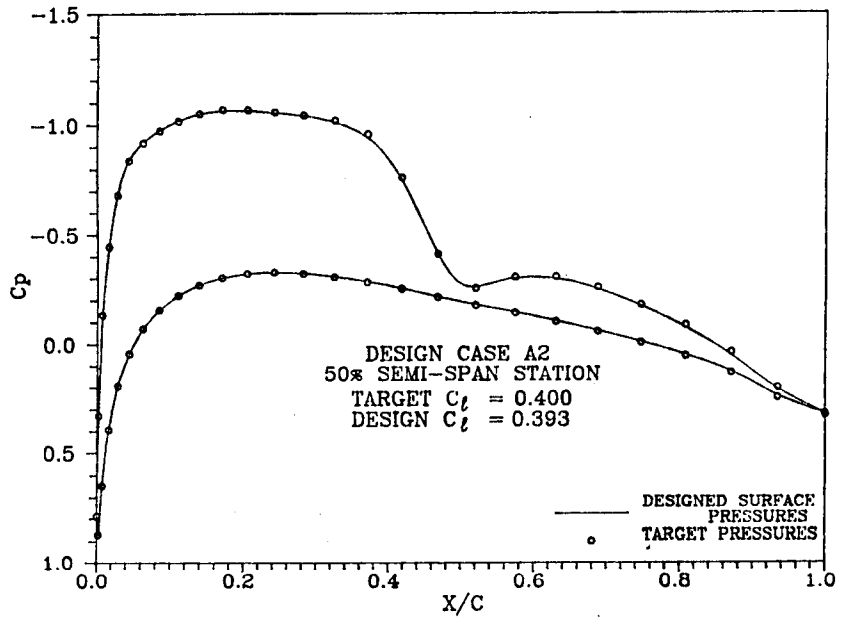

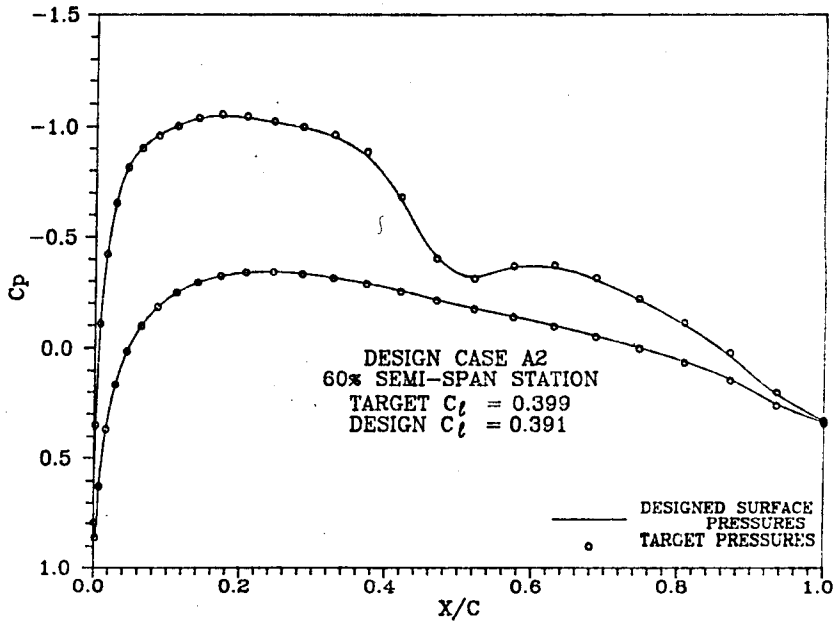

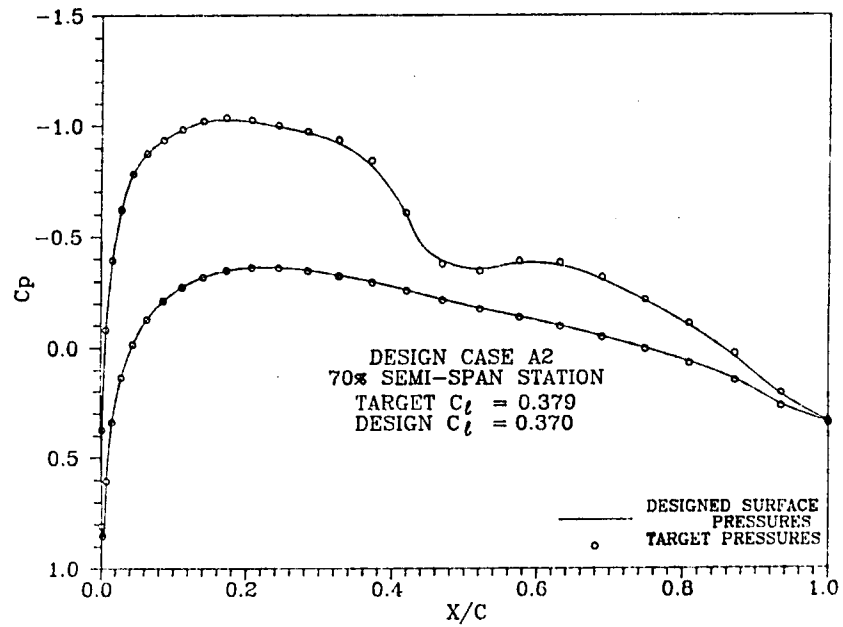

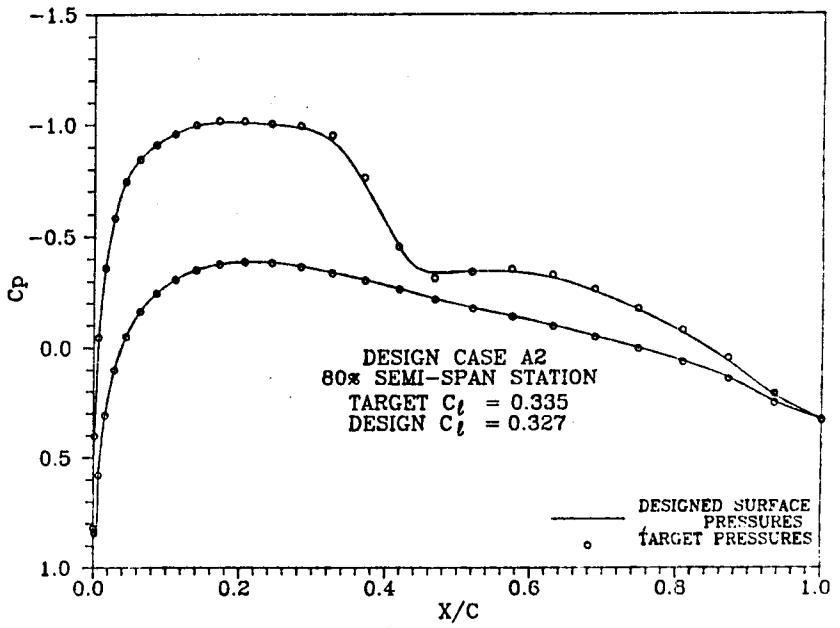

Figure 7 -- Inverse Design Regions for Case B

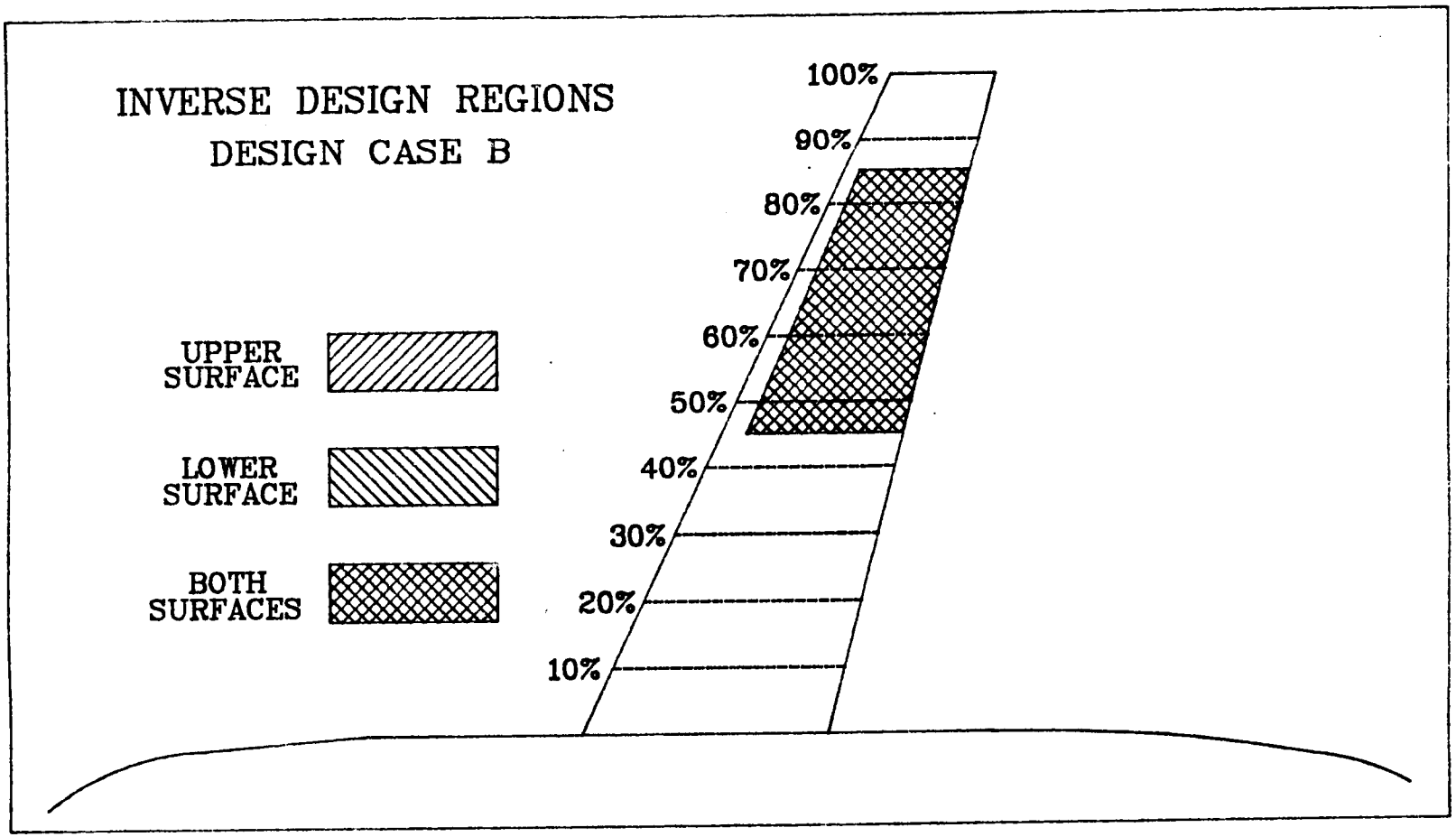

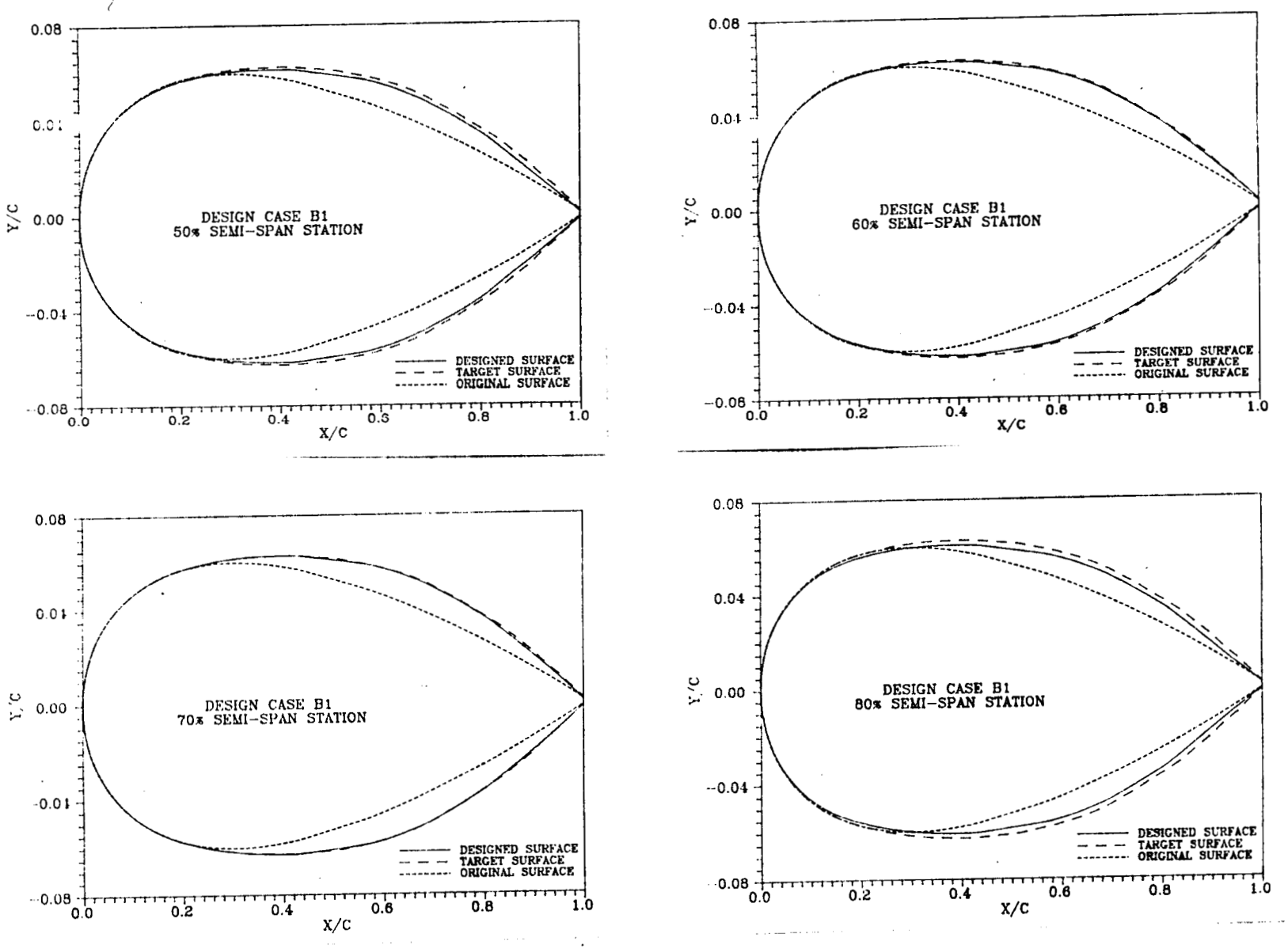

Figure 8 -- Comparison of Designed Sections with Original and Target Sections (Case B1)

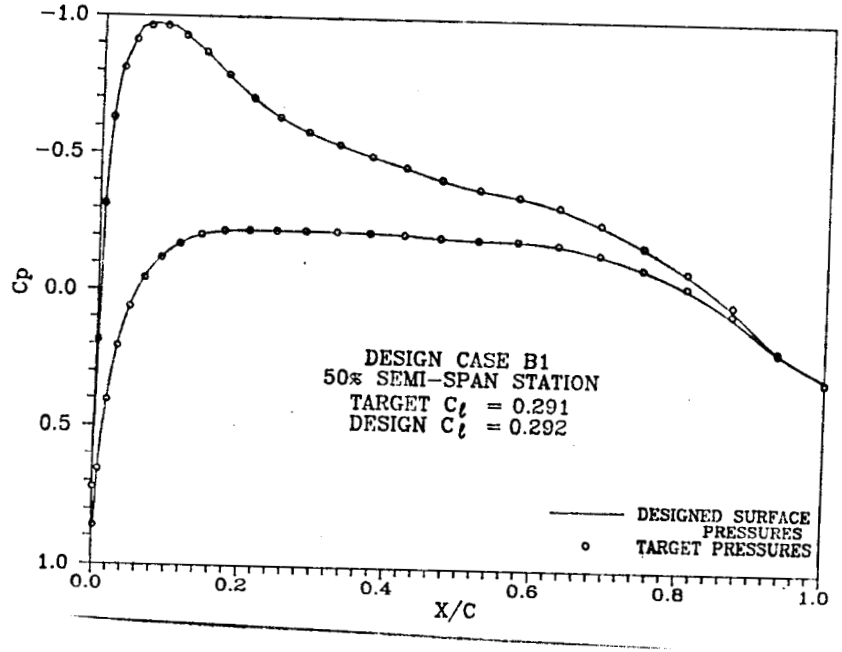

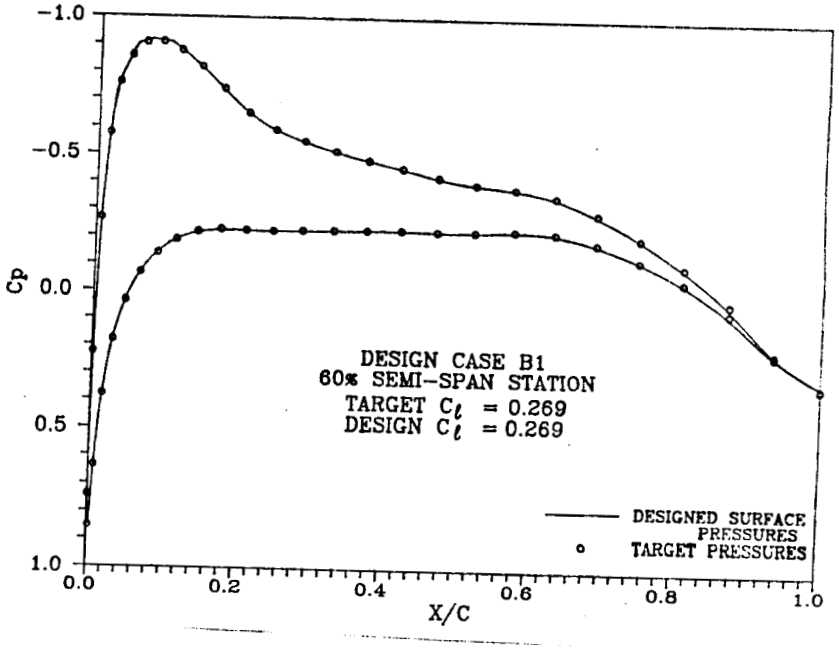

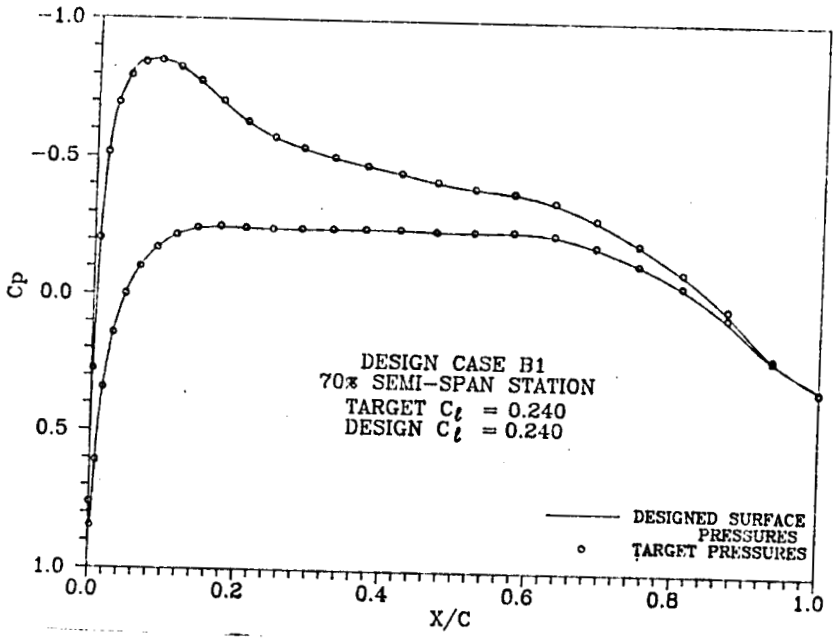

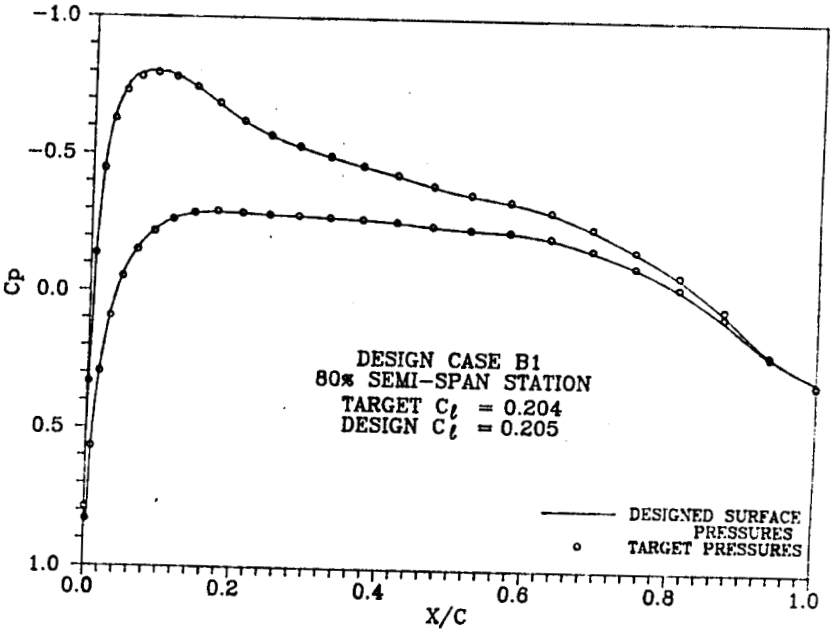

Figure 9 -- Comparison of Pressures from Analysis of Designed Wing with Target Distributions (Case B1)

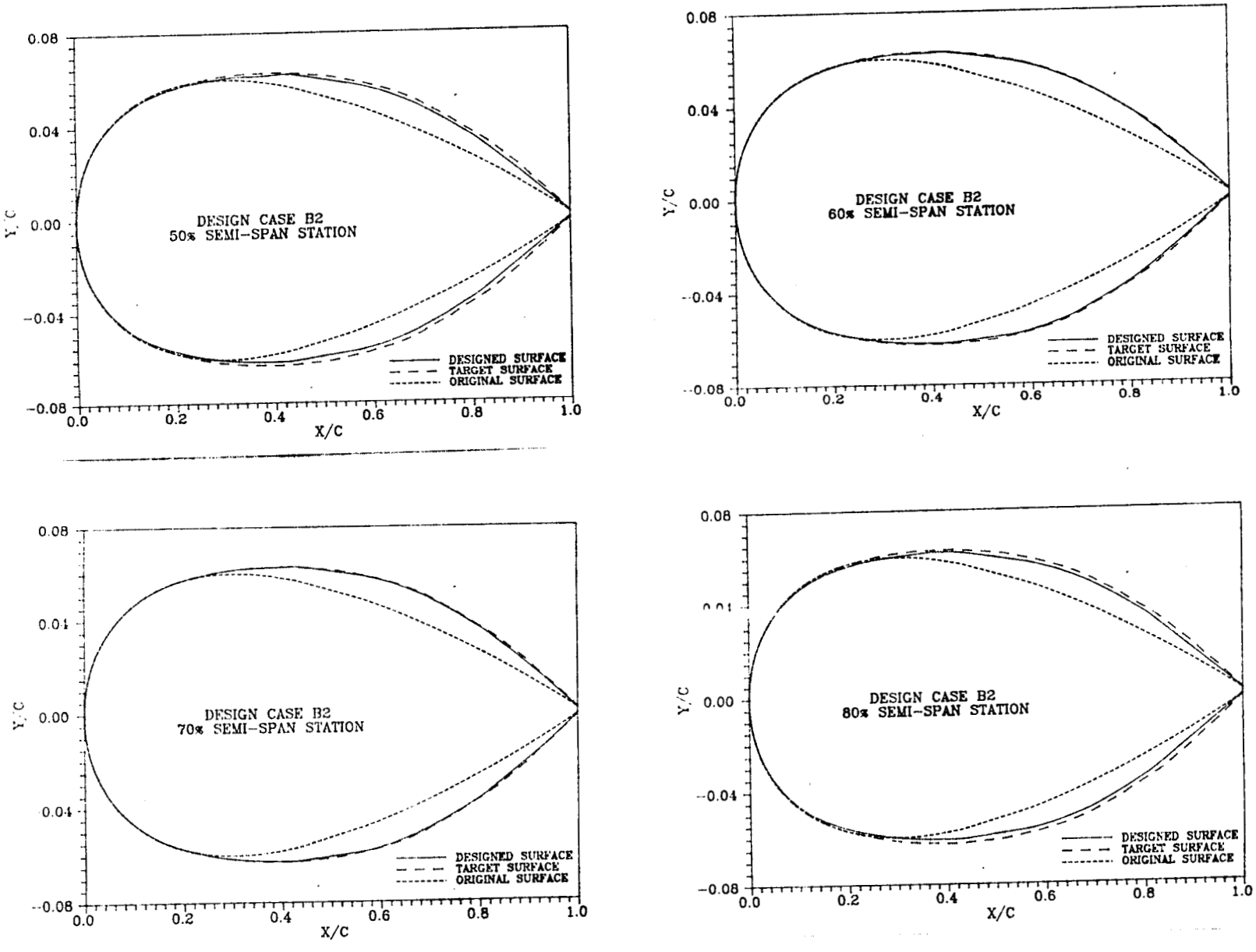

Figure 10 -- Comparison of Designed Sections with Original and Target Sections (Case B2)

Figure 11 -- Comparison of Pressures from Analysis of Designed Wing with Target Distributions (Case B2)

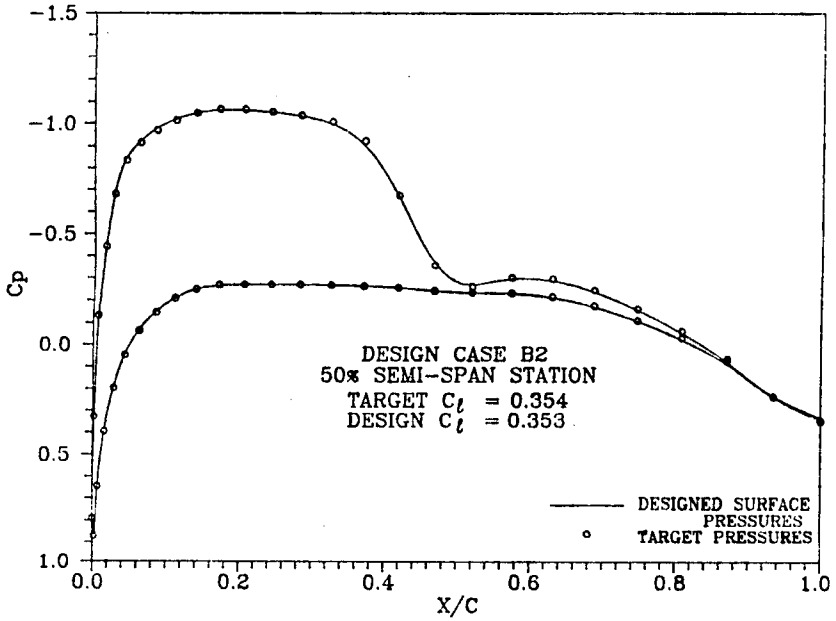

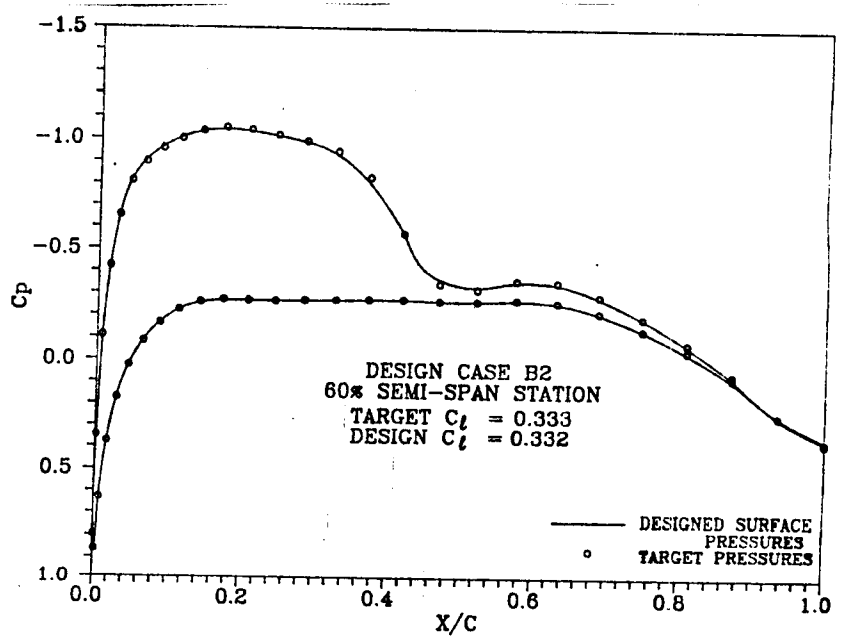

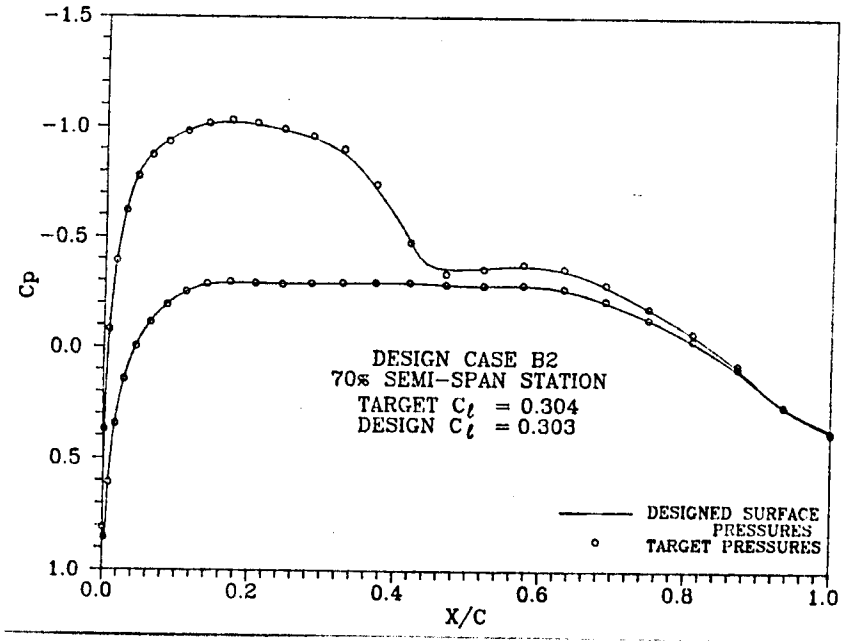

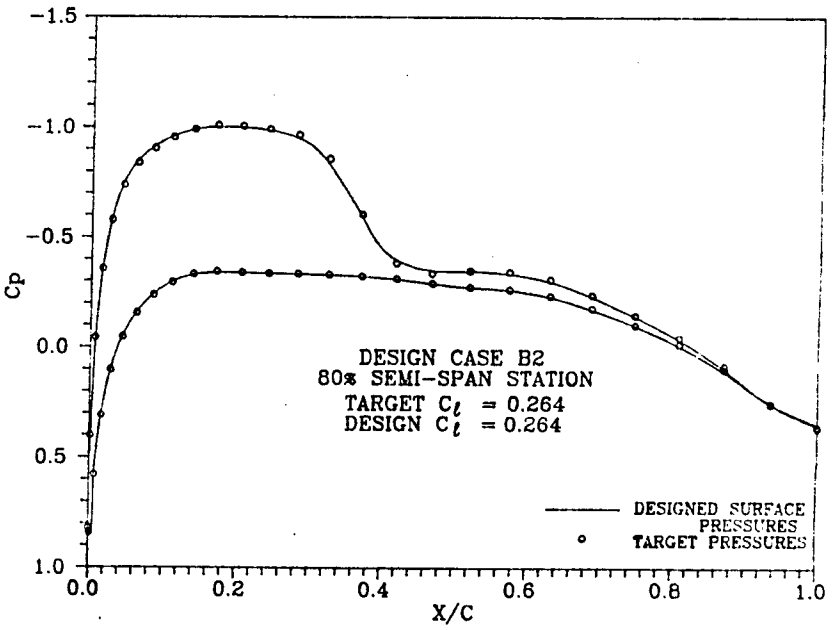

Figure 12 -- Inverse Design Regions for Case C

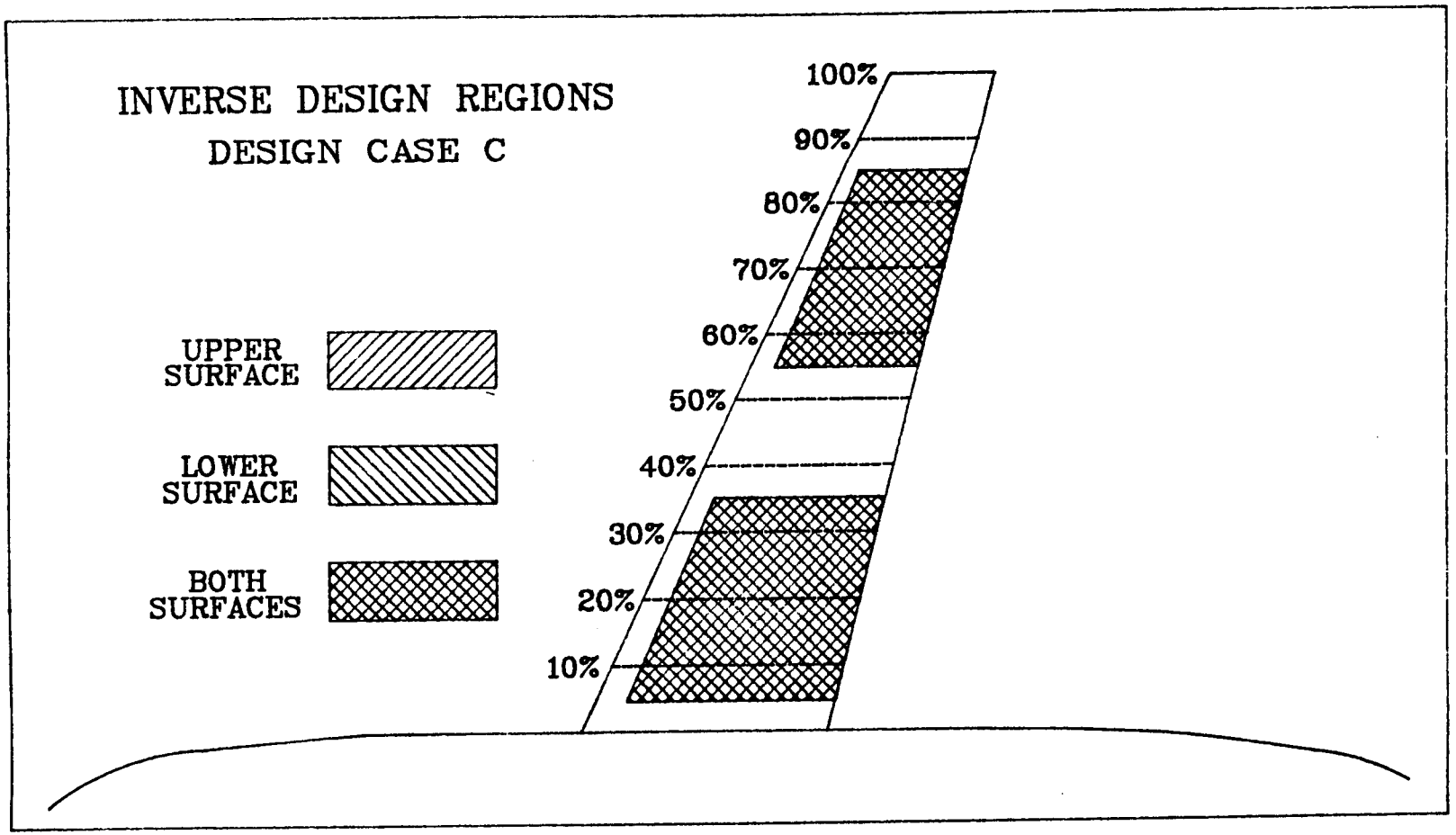

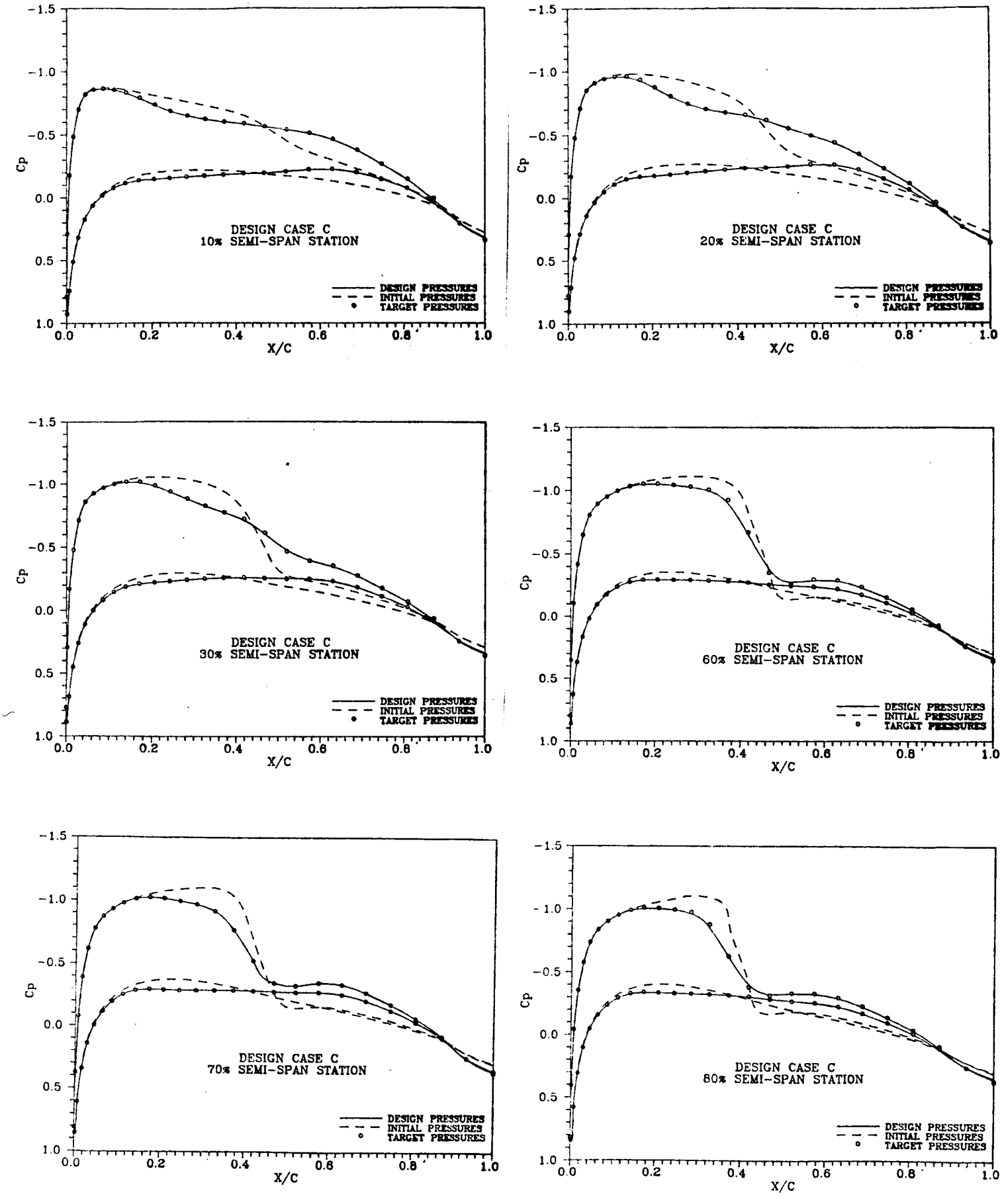

Figure 13 -- Comparison of Initial Pressures with Target Values
(Case C)

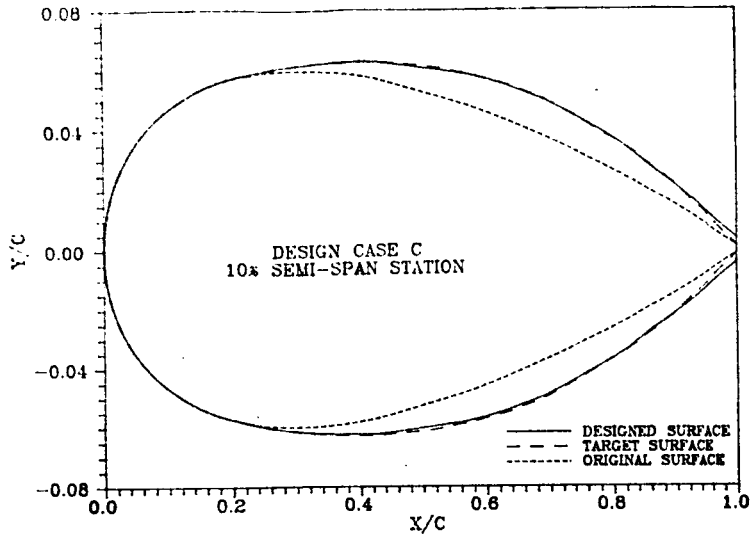

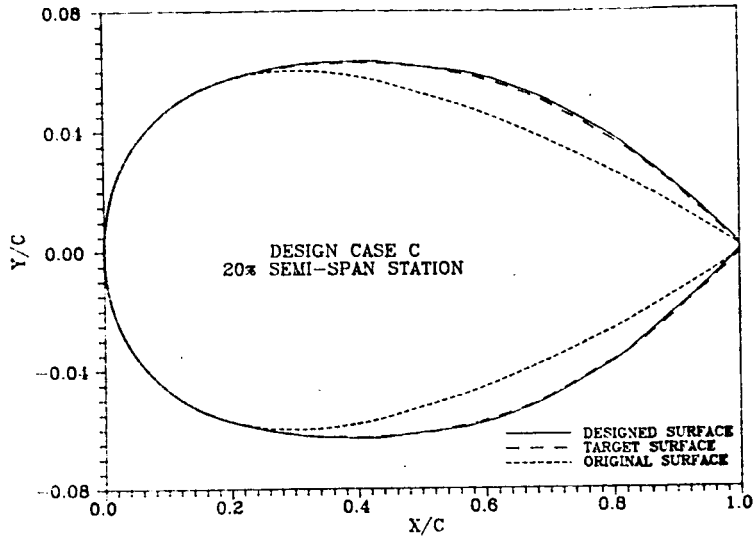

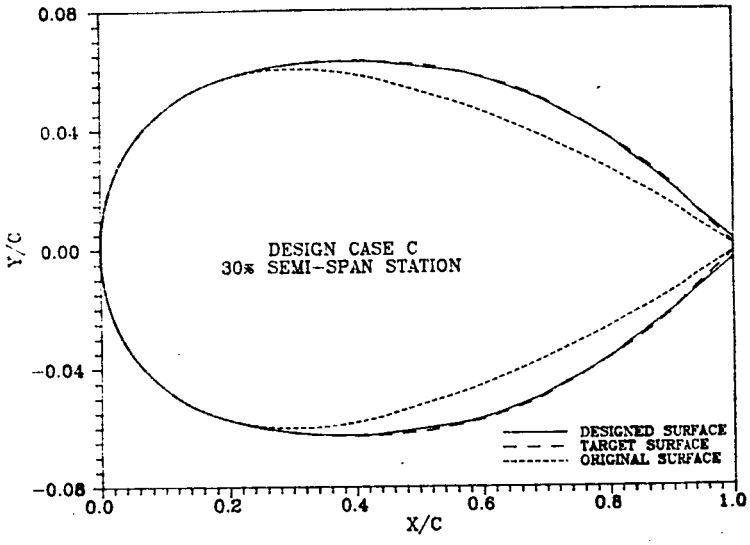

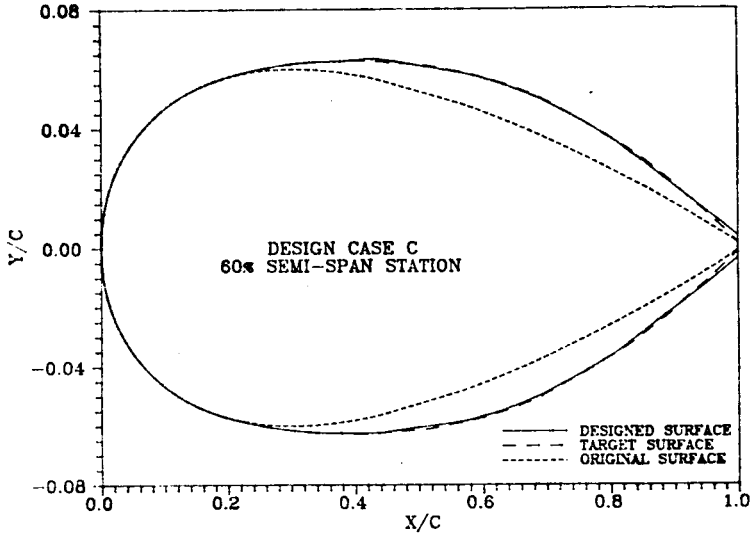

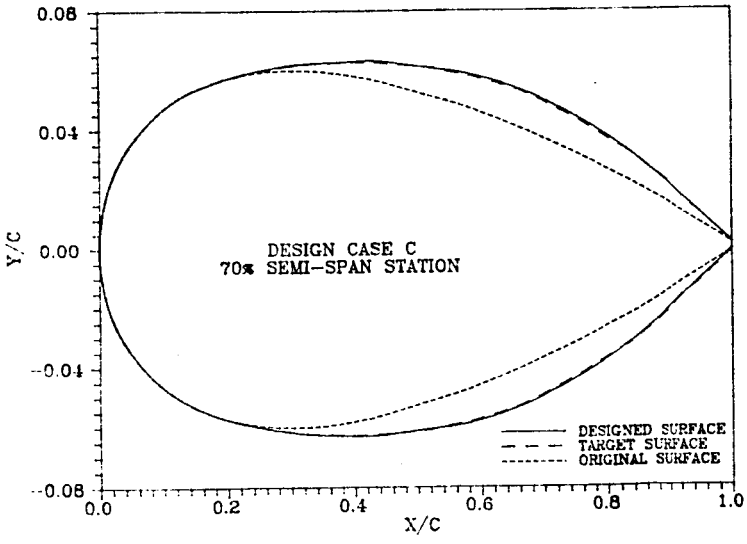

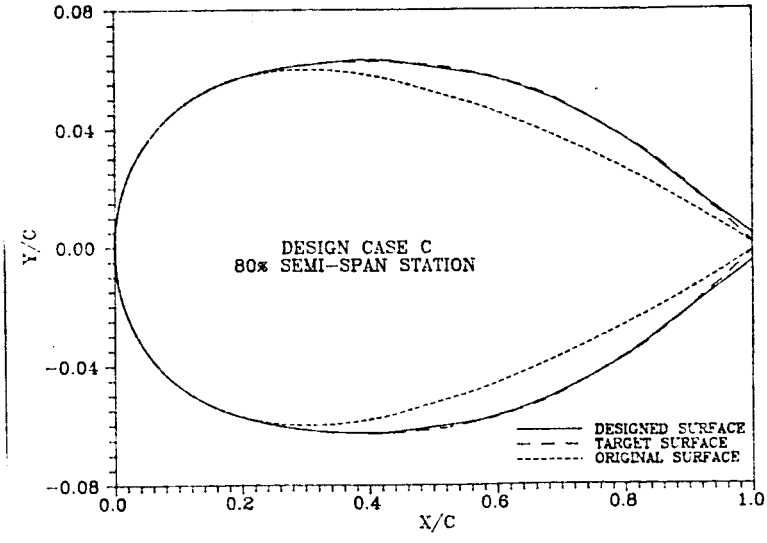

Figure 14 -- Comparison of Designed Sections with Original and Target Sections (Case C)

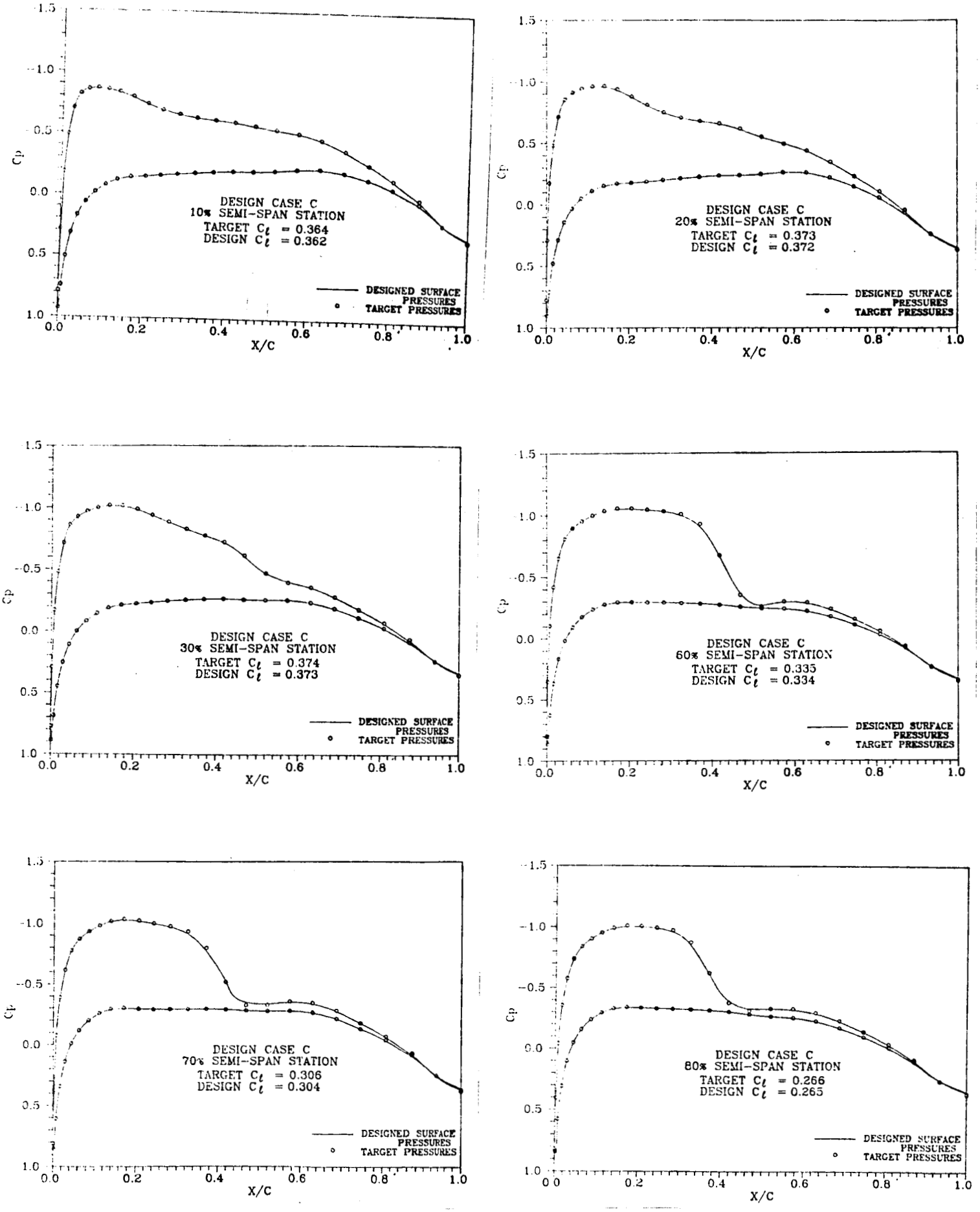

Figure 15 -- Comparison of Pressures from Analysis of Designed Wing with Target Distributions (Case C)

Figure 16 -- Inverse Design Regions for Case D

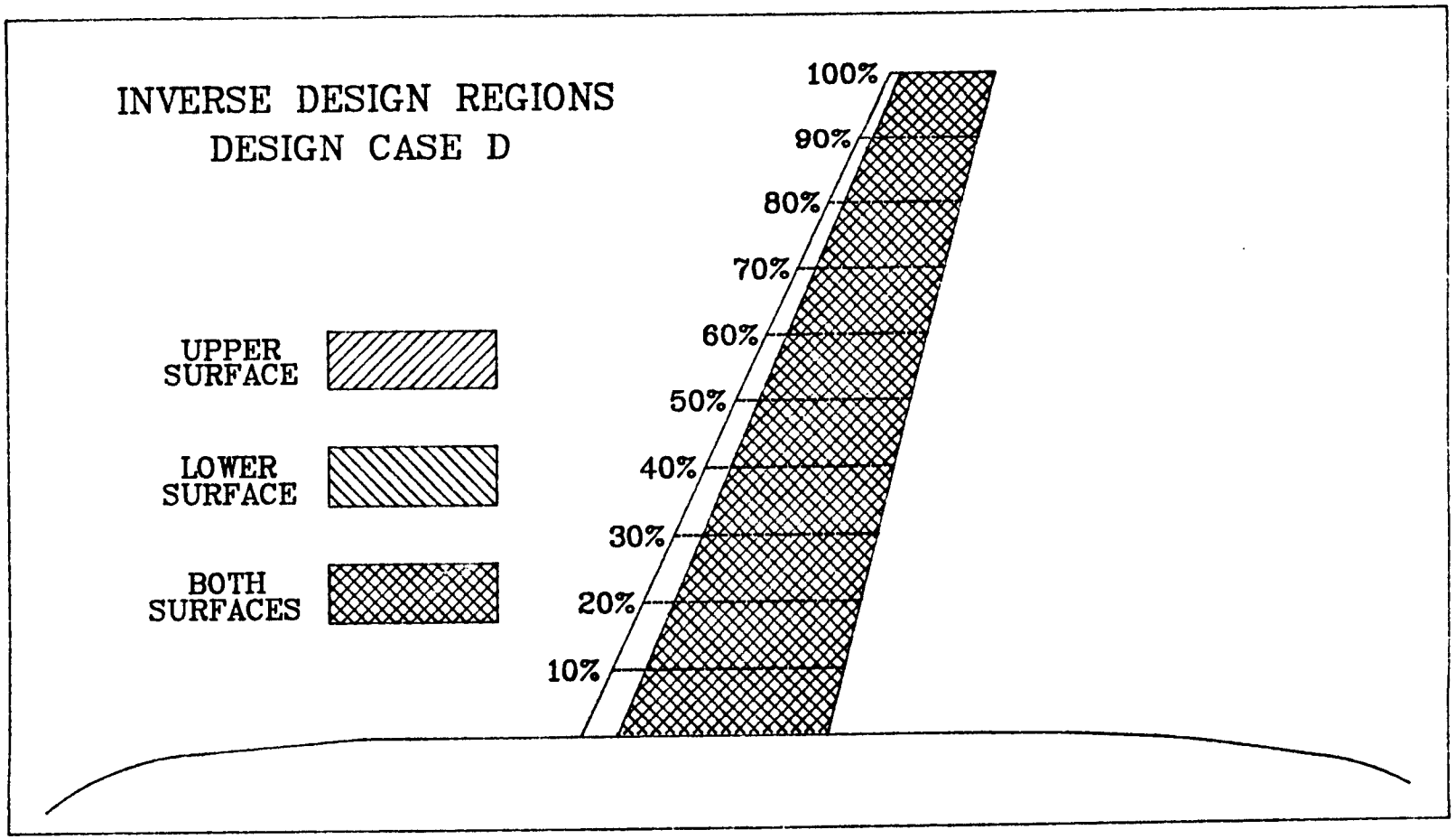

Figure 17 -- Comparison of Initial Twist with Final Twist Distribution

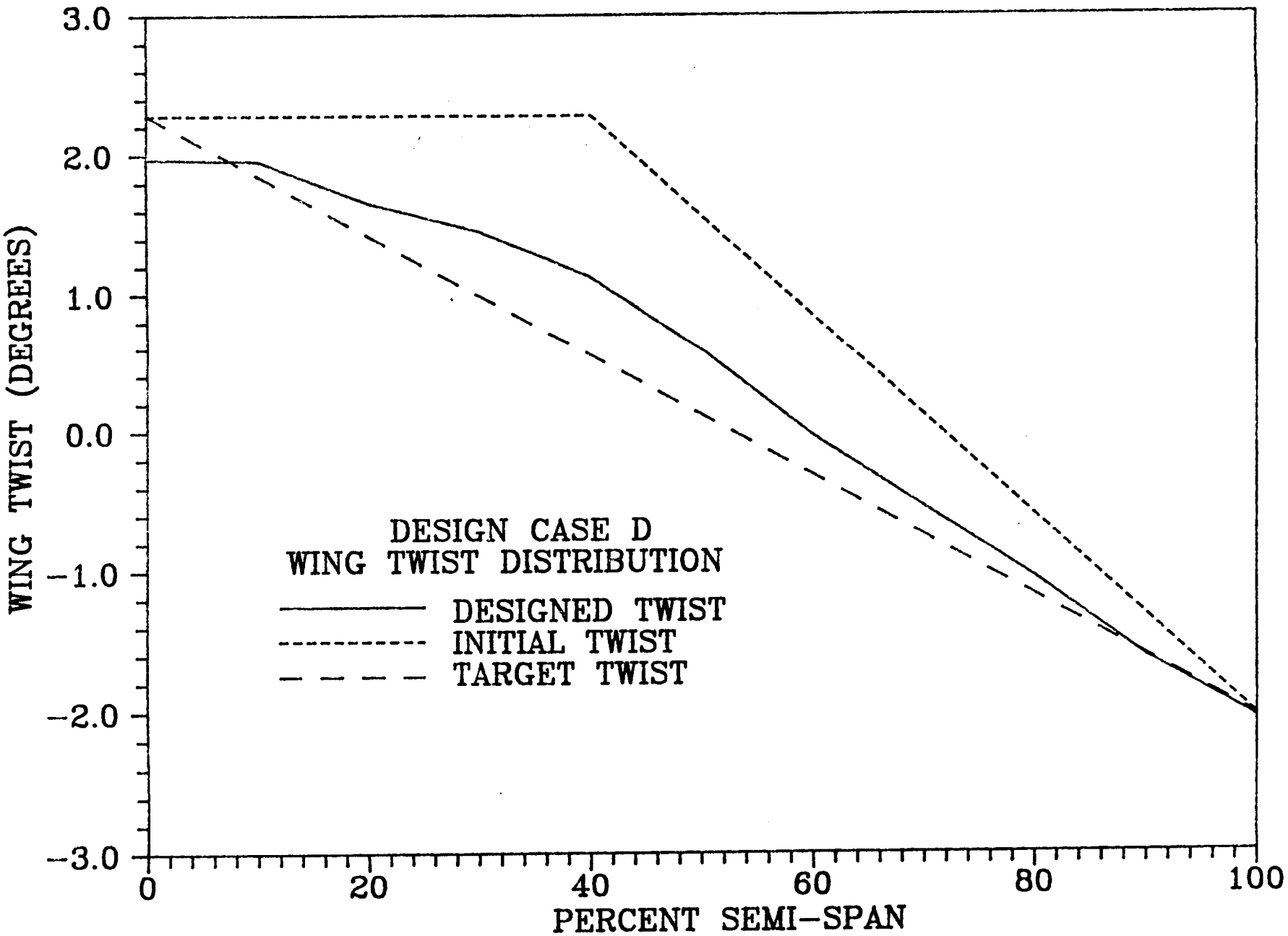

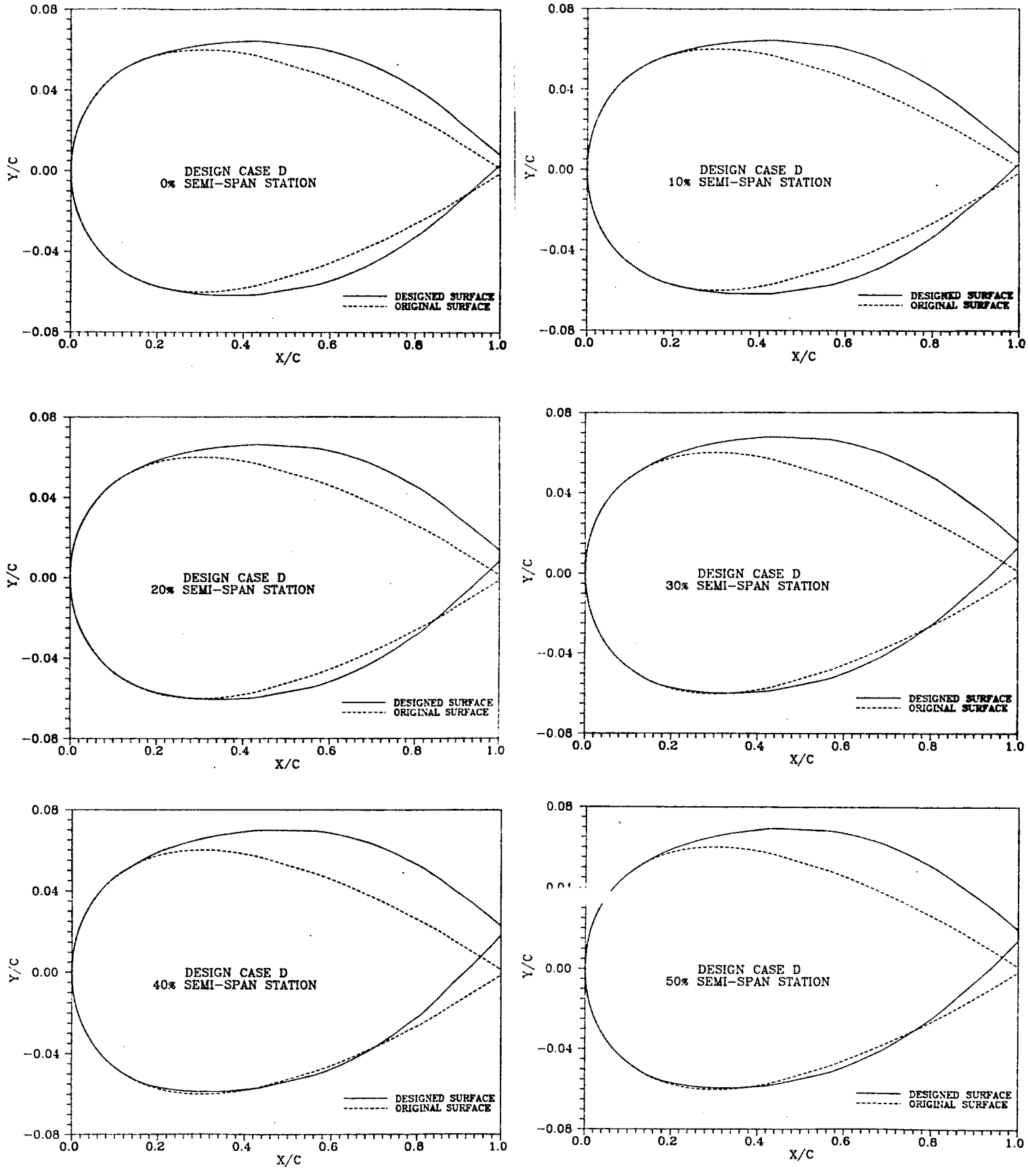

Figure 18(a) -- Comparison of Design Sections with Original Sections (Case D)

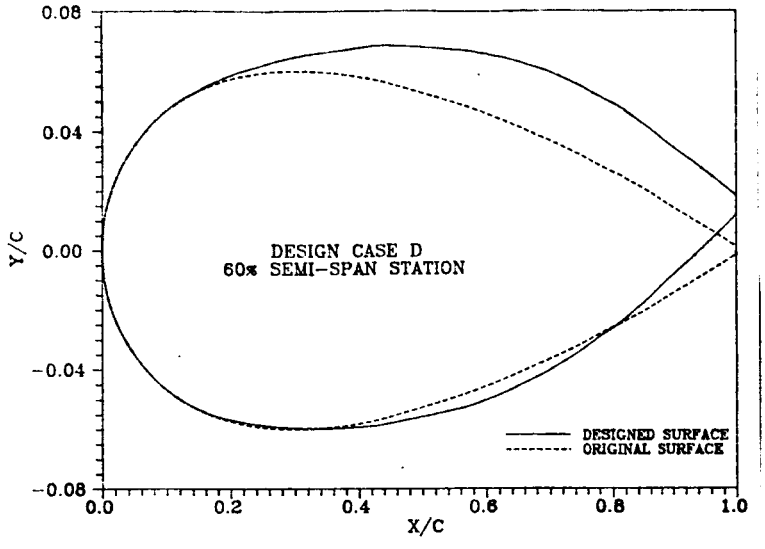

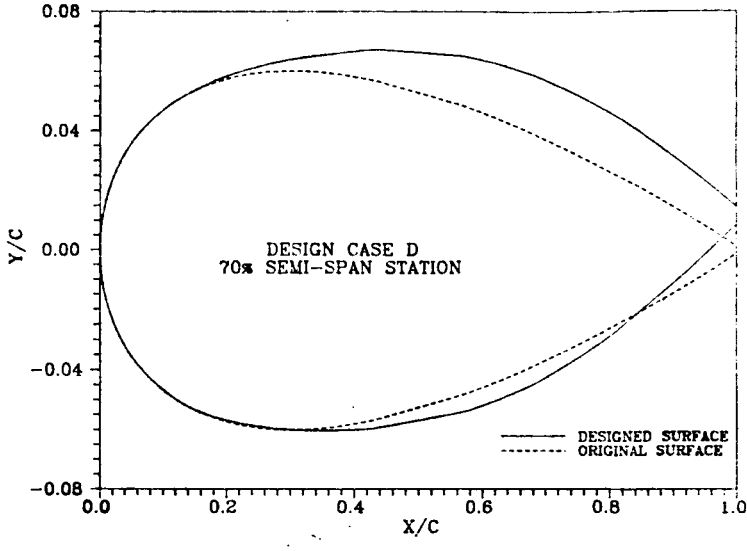

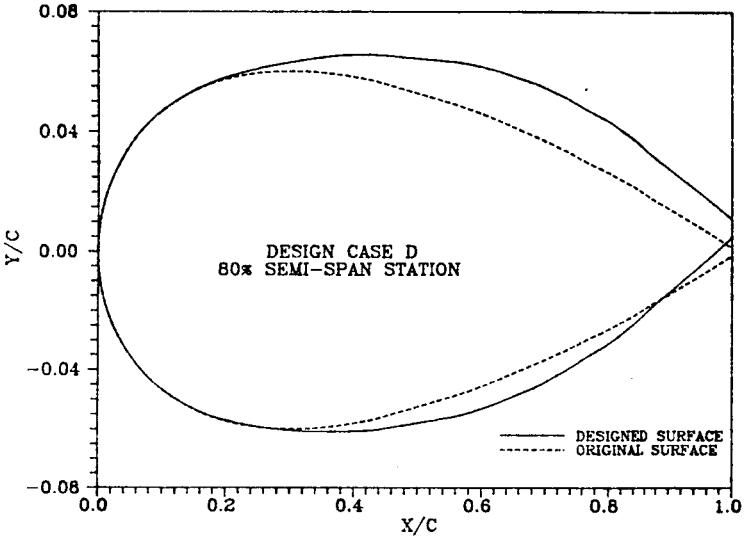

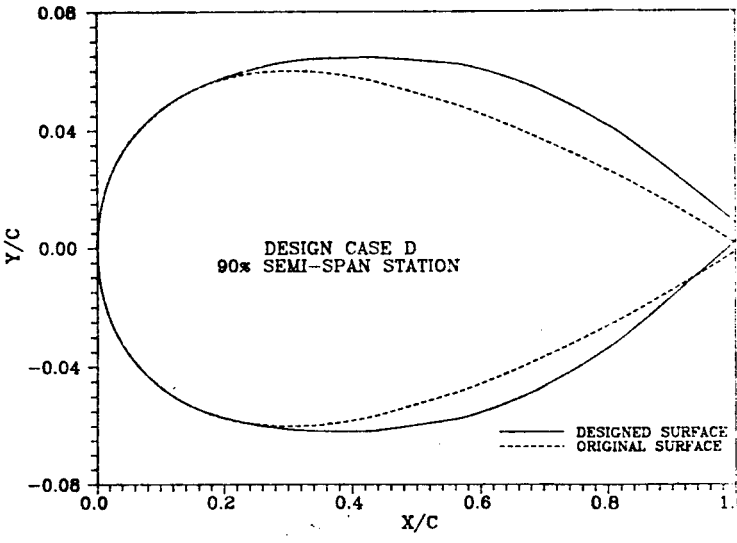

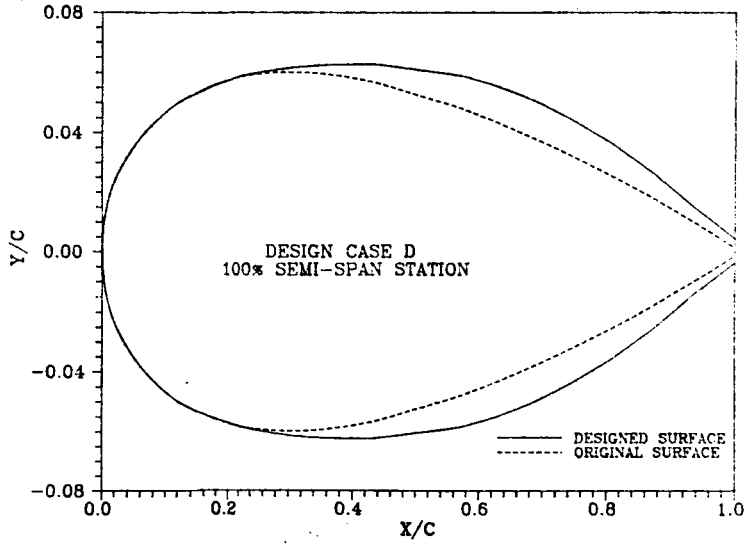

Figure 18(b) -- Continued

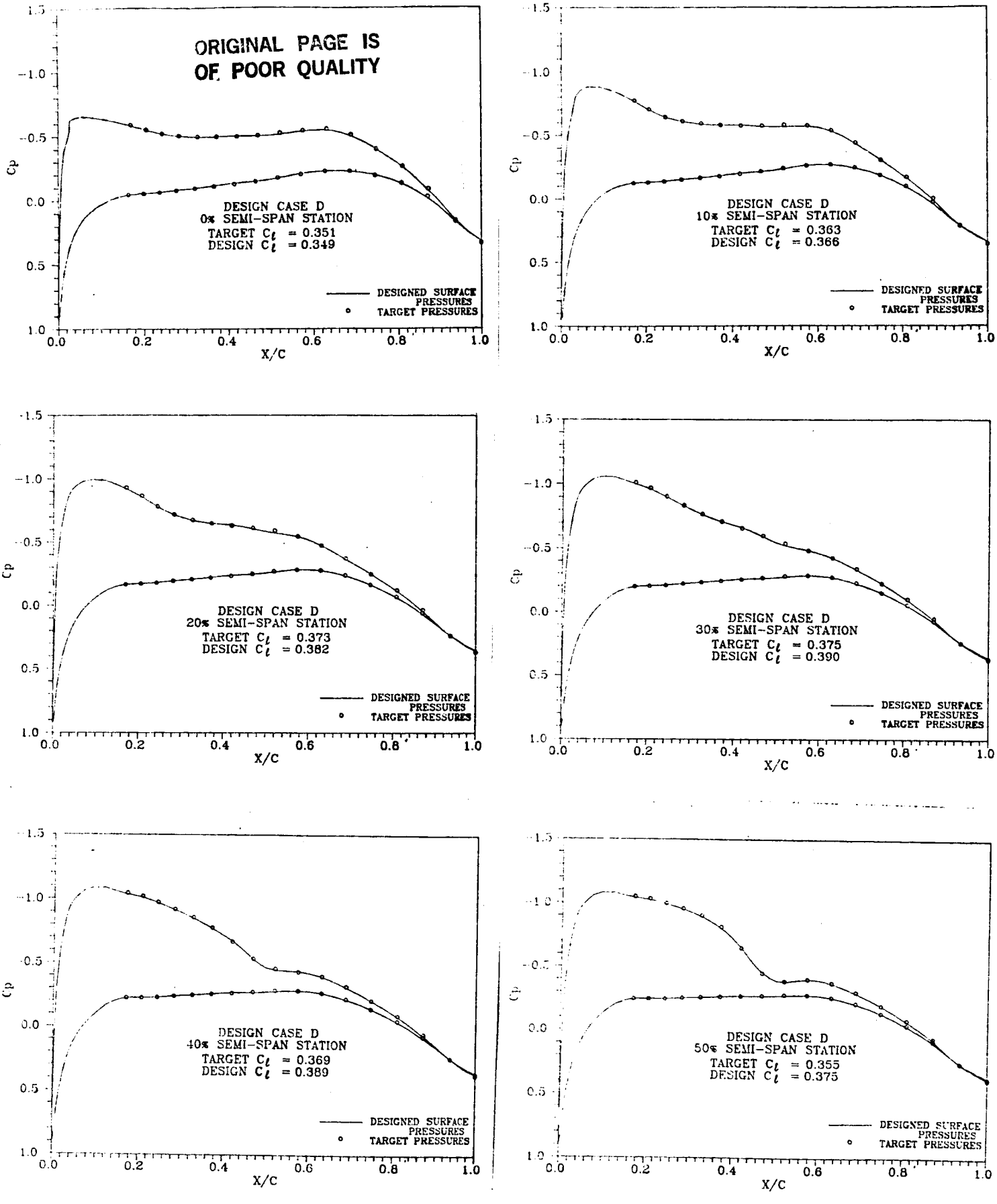

Figure 19(a) -- Comparison of Pressures from Analysis of Designed Wing with Target Distributions (Case D)

Figure 19(b) -- Continued

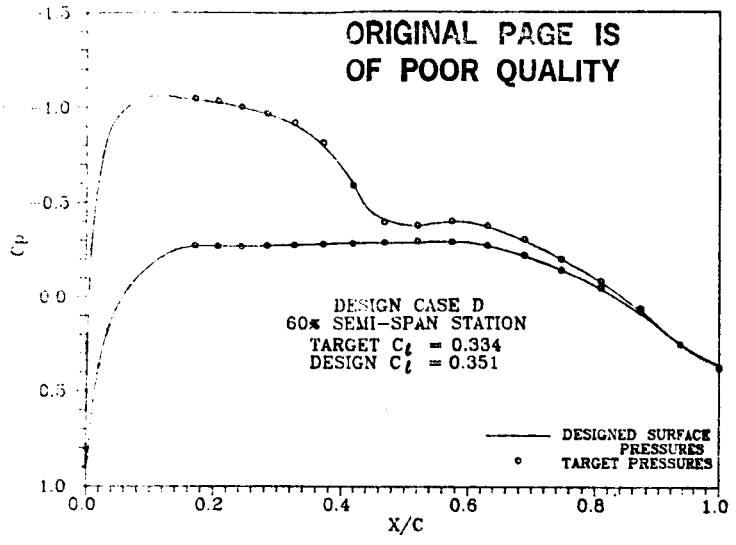

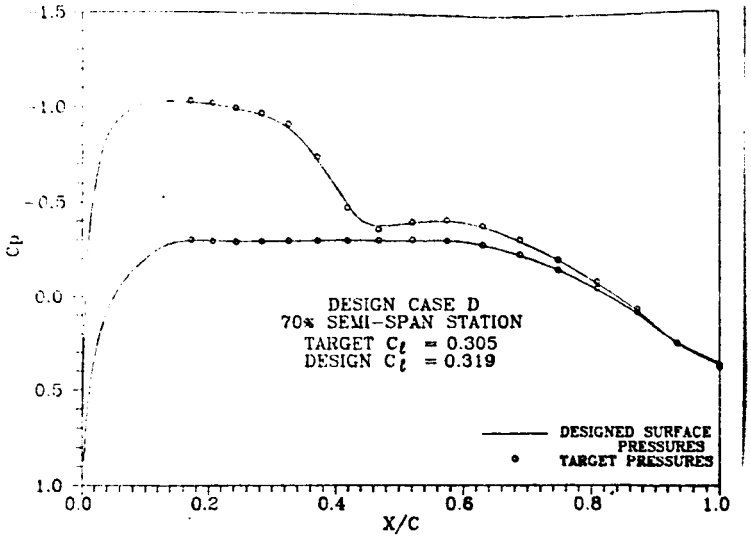

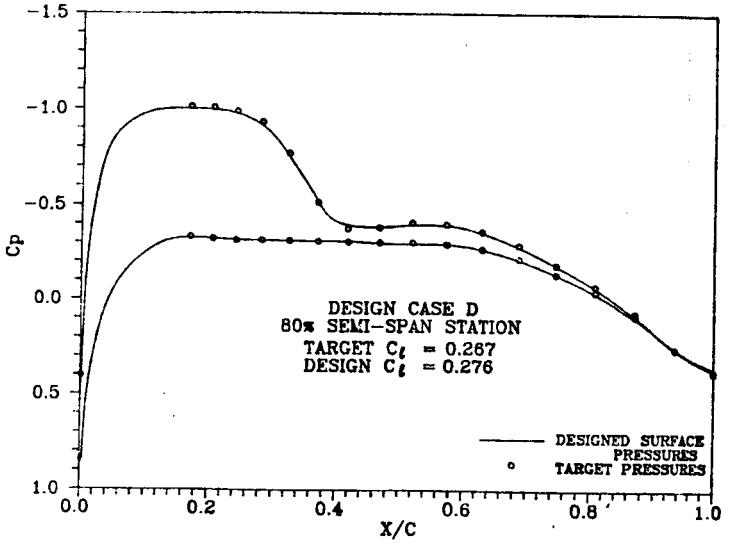

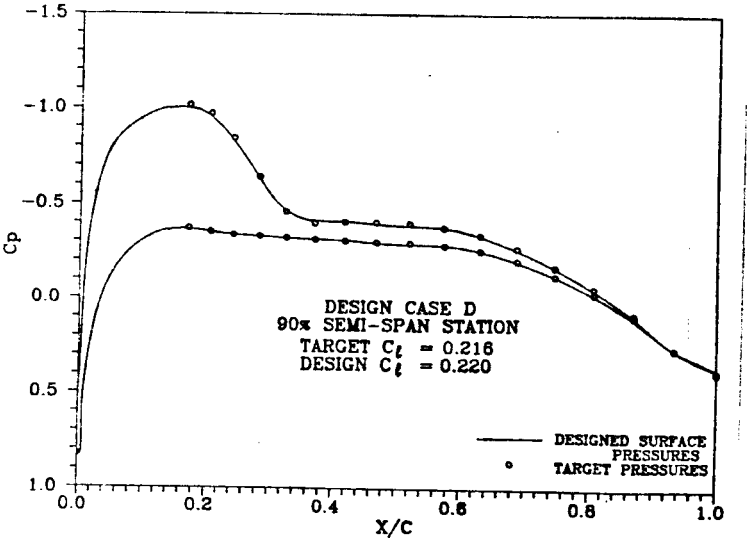

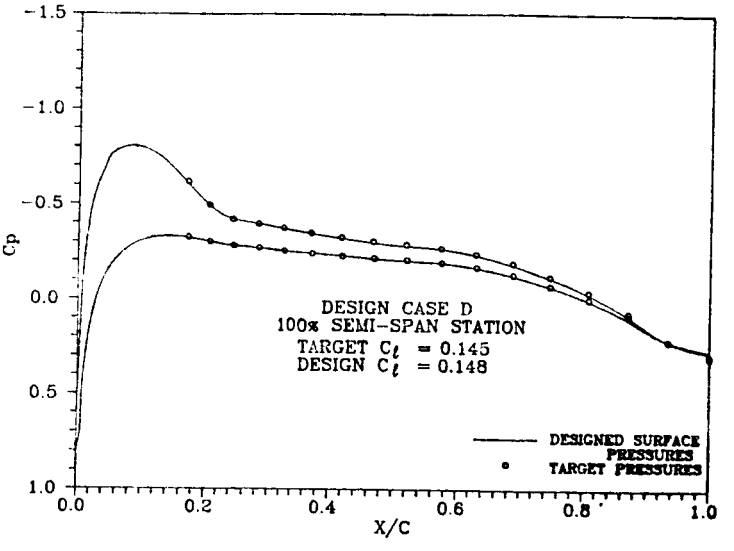

Figure 20 -- Inverse Design Regions for Case E

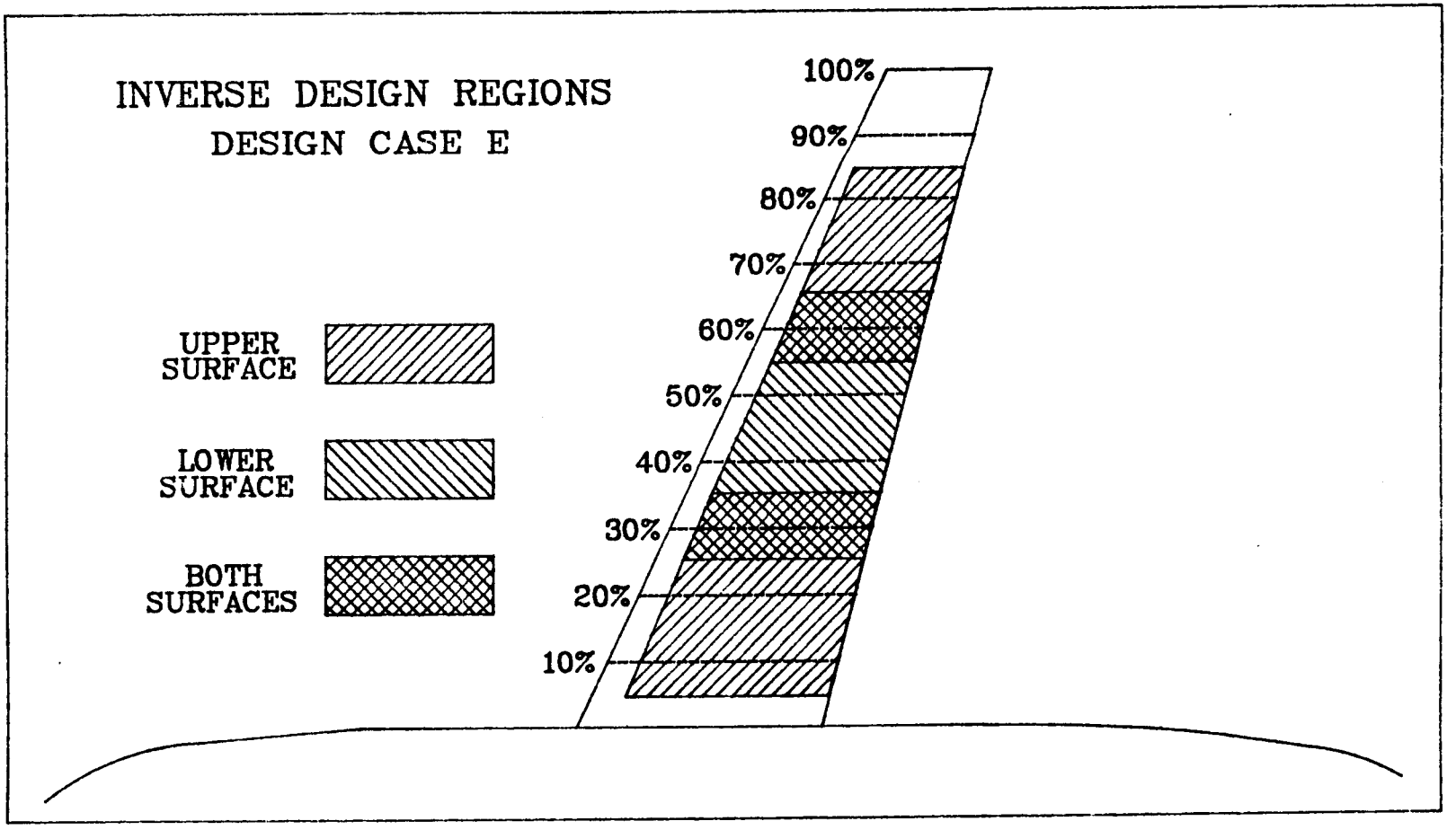

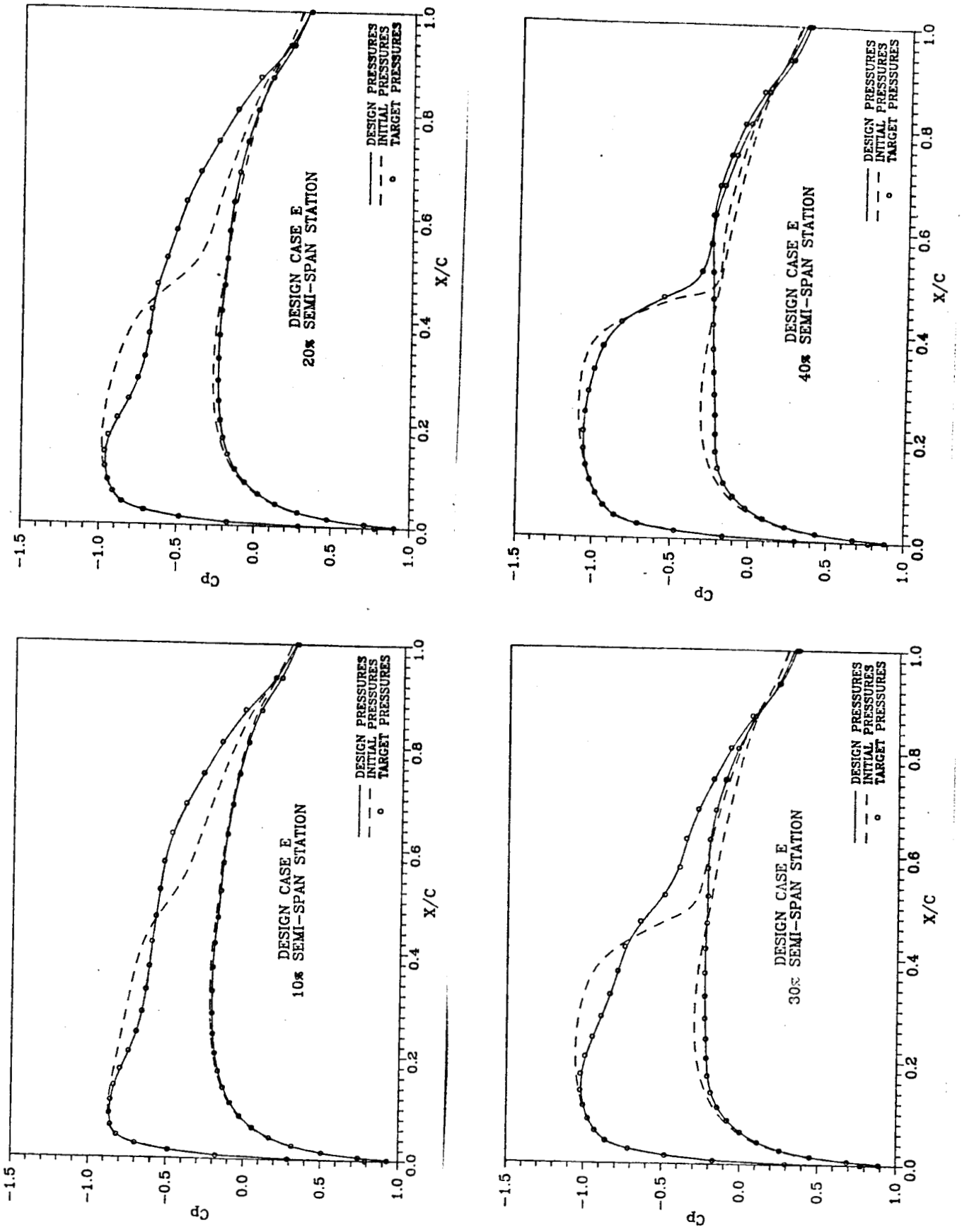

Figure 21(a) -- Comparison of Initial Pressures with Target Values
(Case E)

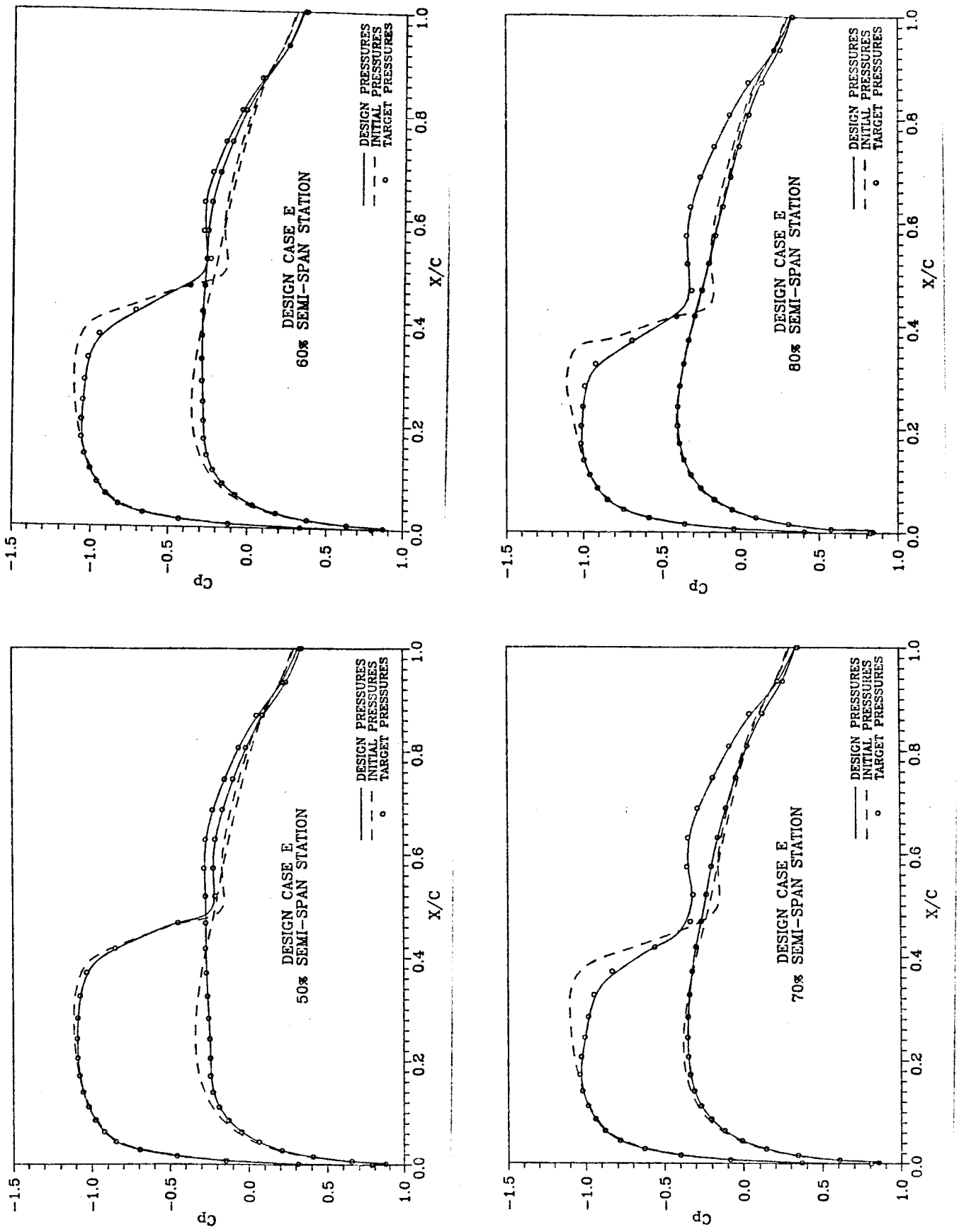

Figure 21 (b) -- Continued

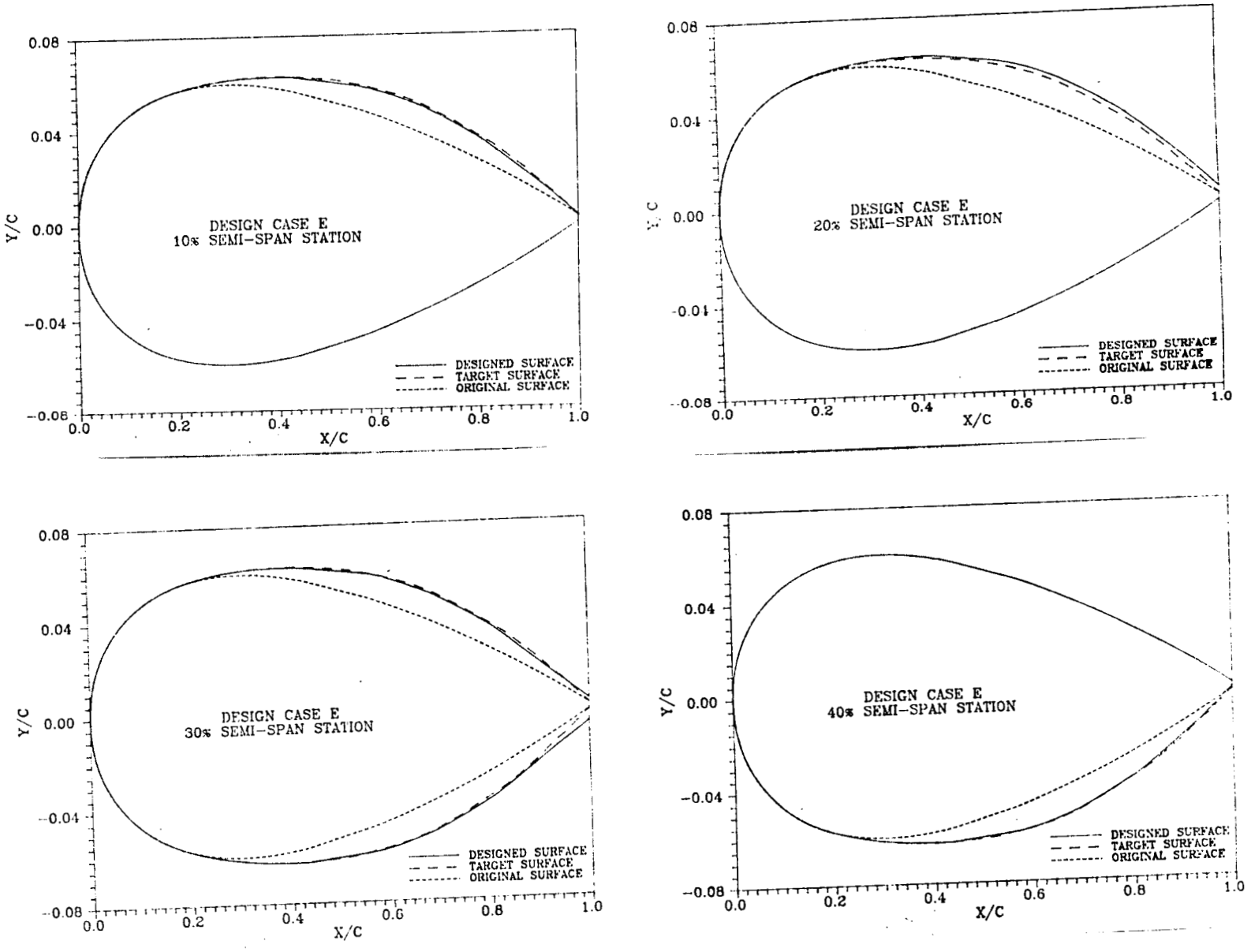

Figure 22(a) -- Comparison of Designed Sections with Original and Target Sections (Case E)

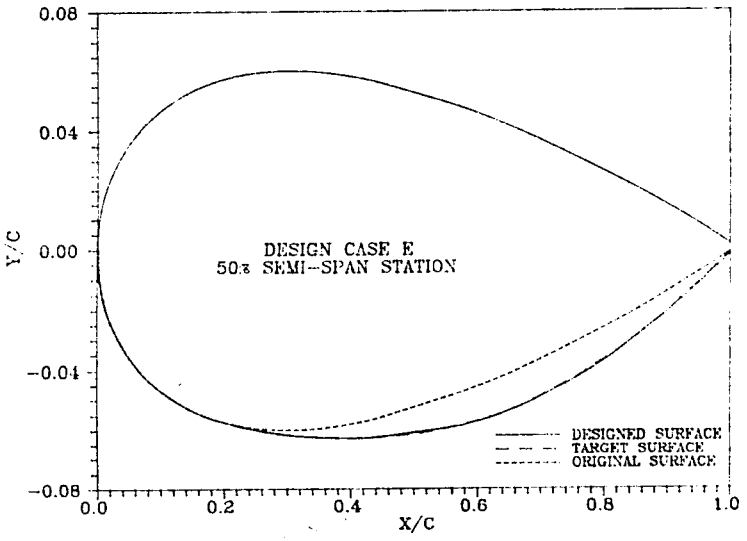

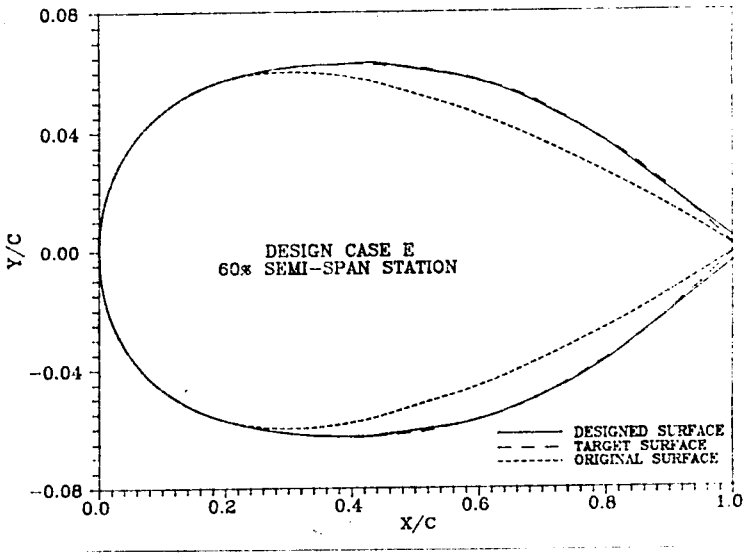

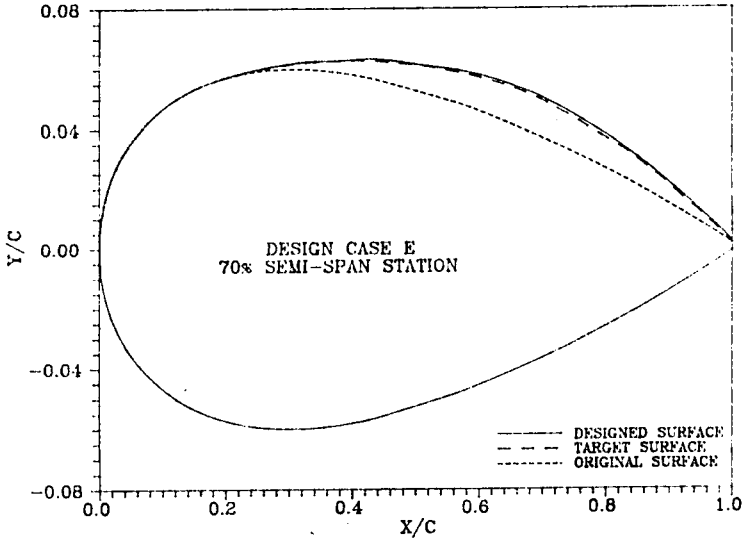

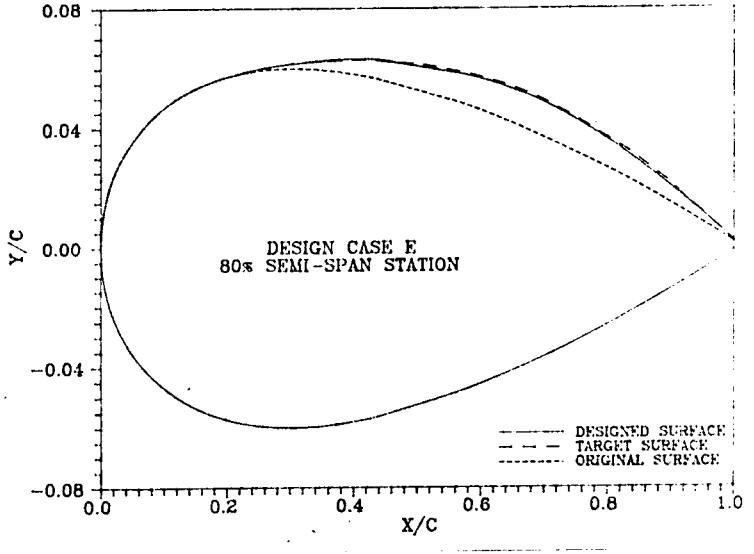

Figure 22(b) -- Continued

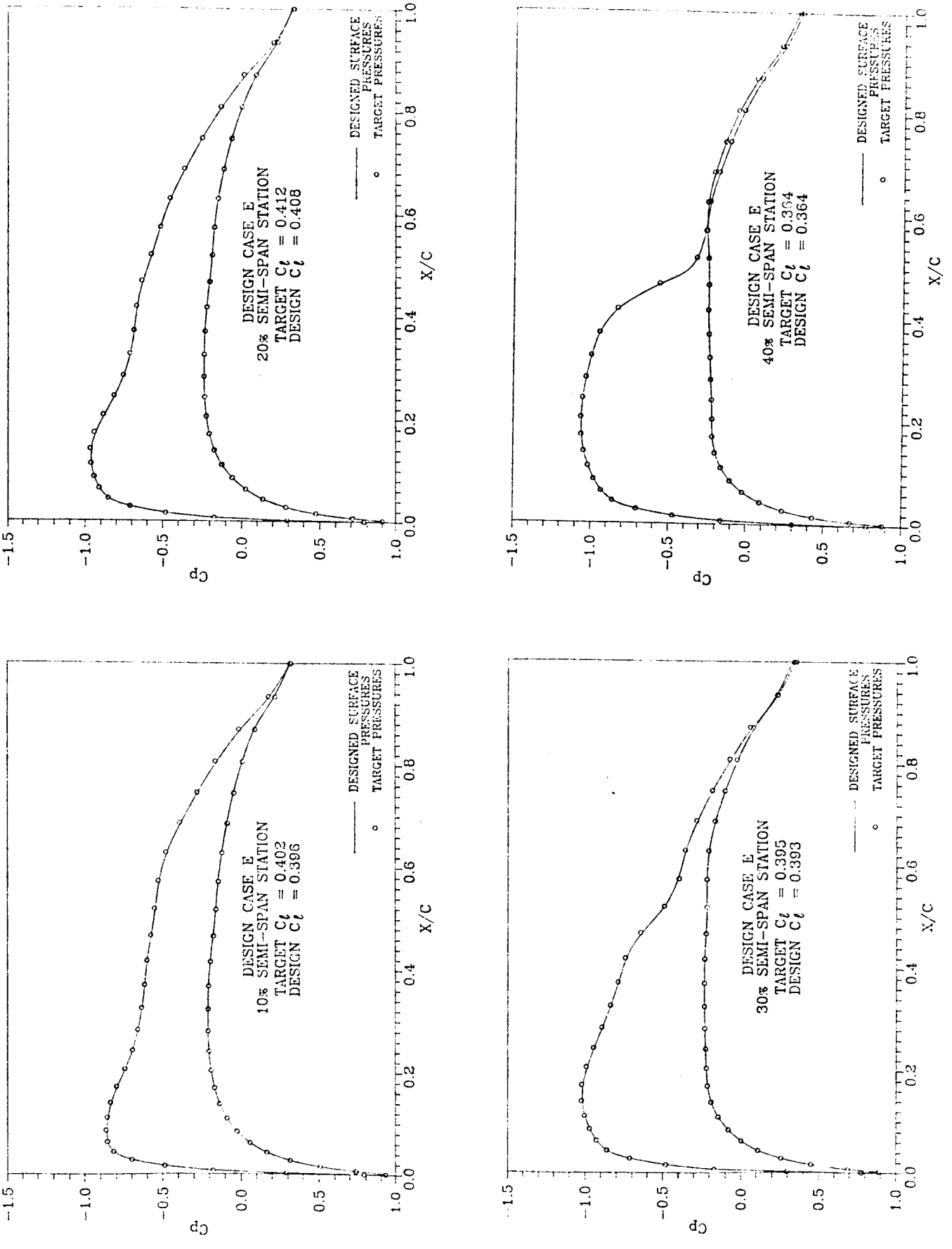

Figure 23(a) -- Comparison of Pressures from Analysis of Designed Wing to Target Values (Case E)

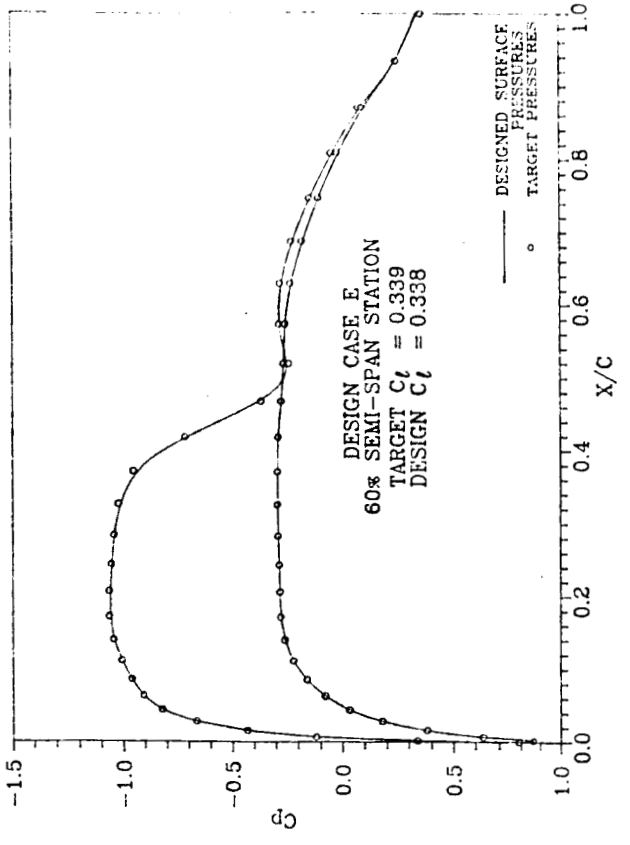

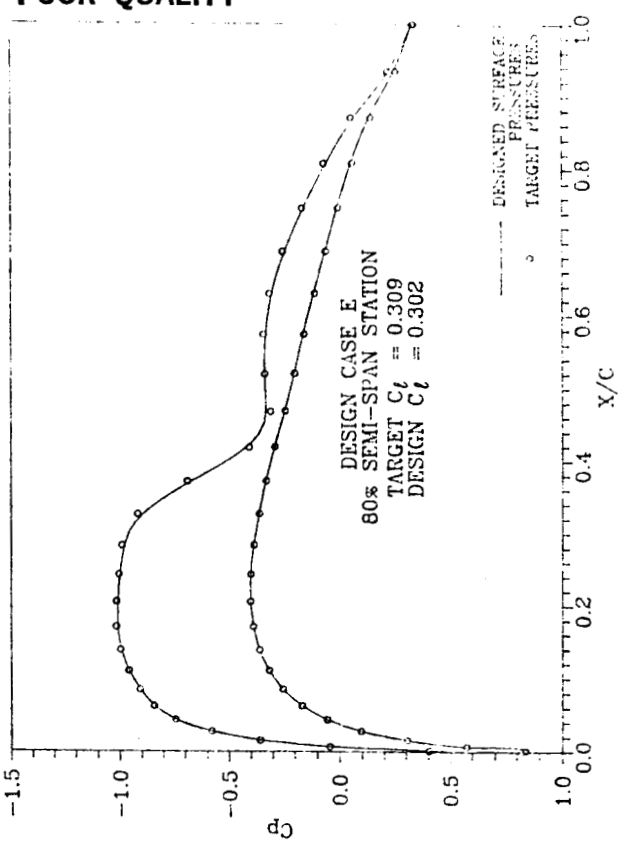

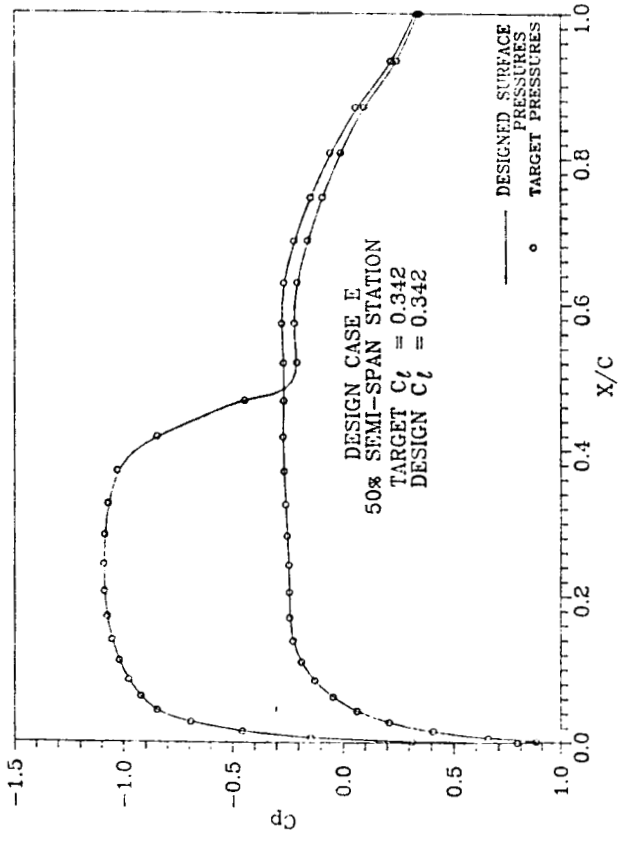

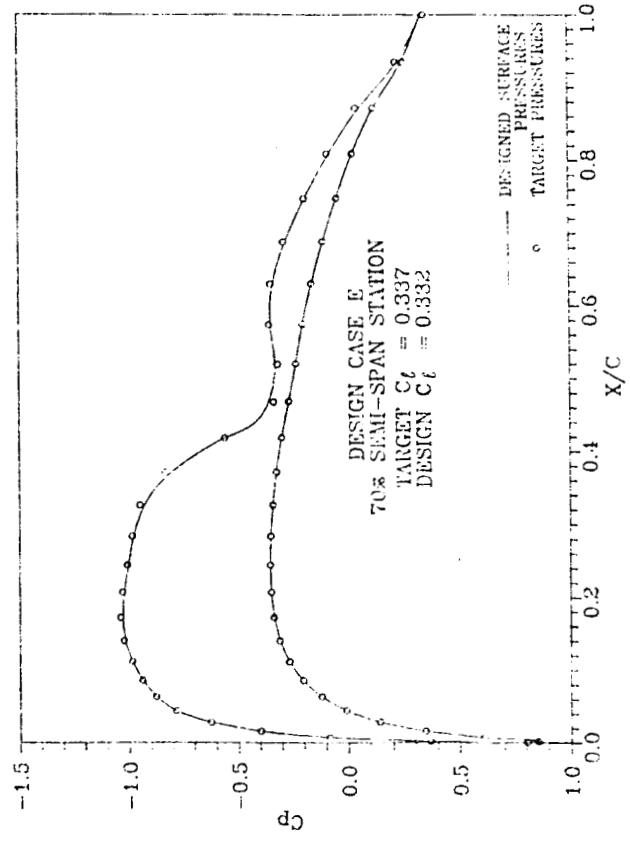

Figure 23(b) -- Continued